# Sukkur IBA
# Journal of
# Emerging Technologies

**Sukkur IBA Journal of Emerging Technologies (SJET)** is the bi-annual research journal published by **Sukkur IBA University**, Pakistan. **SJET** is dedicated to serve as a key resource to provide applied engineering research associated with the Electrical, Electronics and innovations in Energy at the global scale. This Journal publishes manuscripts which are well written by highlighting development in emerging technologies. This Journal covers all branches of Engineering, Science & Emerging Technologies.

**Disclaimer:** The research material expressed in **Sukkur IBA Journal of Emerging Technologies (SJET)** is sole contribution of the authors. The research contribution of the authors does not reflect the management, advisory board, the editorial board, **Sukkur IBA University** press and the organization to which the authors are affiliated. Manuscripts published in **SJET** shall be processed through double-blind peer-reviewed by the two experts of field. The identities of the experts/reviewers shall remain anonymous to the authors. The Journal shall be published two issues in a year. Neither the **Sukkur IBA University** nor the **SJET** shall be responsible for errors or any consequences highlighted by the reader. The errors and deficiencies in terms of research in manuscript can directly be reported to the authors.

*Mission Statement*

The mission of **Sukkur IBA Journal of Emerging Technologies (SJET)** is to provide a premier interdisciplinary platform to researchers, scientists and practitioners from the field of engineering in particular, electrical, electronics, renewable and emerging engineering fields for dissemination of their finding and to contribute in the knowledge domain.

**Aims & Objectives**

**Sukkur IBA Journal of Emerging Technologies (SJET)** will publish and encourage the submission of critically reviewed manuscripts on the cutting-edge research in the field of emerging engineering technologies.

The objectives of **SJET** are:

1. To bring new engineering ideas, research and findings on a single platform.
2. To integrate interdisciplinary research for technological sustainable solution.
3. To provide scholarly platform to connect academia and industries for socio-economic development.

*Research Themes*

The research focused on but not limited to following core thematic areas:

**Renewable Energy Sources and Storage:**

- Solar energy system fabrication and construction of advanced fuel cell technology
- Designing and analyzing smart hydro and wind energy systems
- Developing systems for biomass and bio-fuels
- Energy management and storage
- Energy devices and materials
- Energy harvesting for wireless and body sensor networks
- Energy efficiency and policies
- Energy devices and materials

**Power Systems and Smart Grids:**

- Power Quality Issues and solutions
- Micro grid systems and their Integration Problems

- Design control and management
- Energy management and Environmental issues
- Hybrid power system
- Distributed and co-generation systems
- Power market and power system economics

**Electrical Machines and Adjustable Speed Drives:**

- AC and DC machines and drives
- Sensor-less control
- Piezo and electrostatic actuators
- Machine design and equipment training
- Maintenance and fault diagnosis
- Bearing less driving technologies

## Power Electronics and its Application:

- Hard-switching and soft-switching static converters
- Multi-level and matrix converters
- Emerging topologies
- Simulation and control power converters
- Power factor correctors
- Active filters and total harmonics distortions analysis
- Optoelectronics and photonic devices
- Power semiconductors, passive components, and packaging technologies
- Switch-mode power supplies and automotive
- Applications of power electronics in home appliance

## High Voltage Engineering and Insulation Technology:

- Micro-electromechanical system (MEMS)
- Power Integrated circuits (PIC)
- Power Engineering related Technologies
- Power system stability and control
- Power system transient modeling, simulation and analysis
- Electromagnetic transient programs (EMTP)
- HVDC and FACTS applications

## Nanomaterials/Nanotechnology:

- Sensors and Actuators
- Electronic Thin Films
- Nanogenerators
- Nanomaterials

- Nanotechnology optoelectronic sensors
- magnetic sensors
- thermal sensors
- mechanical sensors

## Communication and Signal Processing:

- Communication & signal processing
- Radio frequency systems, microwave and antenna design
- Analog and mixed signal circuits
- Filter designing
- Satellite communication, mobile communication
- Cognitive and software design radio
- Analog and Mixed Signal Circuits

## Biomedical Electronics:

- Energy-efficient wireless body sensor networks
- Wireless power/energy transfer in e-health applications
- Green and battery-friendly wireless medical networks
- Renewable energy and energy harvesting for wireless and body sensor networks
- Telemedicine and medical IoT
- Medical video transmission
- Energy management for medical health applications
- Role of 5G in medical health applications

## Thermal and complex fluid dynamics:

- Active and passive techniques for fluid flow manipulation

- Fluid flow process for industrial equipment's
- Modeling of working fluids
- Experimental fluid dynamics
- Multifunctional heat exchangers/chemical reactors
- Energy efficient combustion
- Environmental fluid flows

## Materials and their processing

- Piezoelectric materials
- Polymers, metal oxides
- III, V and II, VI semiconductors

- Thick and thin films
- Optical glass fibers
- Amorphous
- Polycrystalline monocrystalline silicon, nanomaterials
- Synthesis of nanomaterials, composite materials
- Functional material
- Electronic thin films and integrated devices
- Engineering materials
- Solid and structural mechanics

# Patron's Message

**Sukkur IBA University** has been imparting education with its core values merit, quality and excellence since its inception. Sukkur IBA University has achieved numerous milestones in a very short span of time that hardly any other university has achieved in the history of Pakistan. The institute continuously being ranked as one of the best Institute in Pakistan by Higher Education Commission (HEC). The distinct service of Sukkur IBA University is to serve rural areas of Sindh and also underprivileged areas of other provinces of Pakistan. Sukkur IBA University is committed to serve targeted youth of Pakistan who is suffering from poverty and deprived of equal opportunity to seek quality education. Sukkur IBA University is successfully undertaking its mission and objectives that lead Pakistan towards socio-economic prosperity.

In continuation of endeavors to touch new horizon in the field of Engineering and Emerging Technologies, Sukkur IBA University publishes an international referred journal. Sukkur IBA University believes that research is an integral part of modern learnings ad development. **Sukkur IBA Journal of Emerging Technologies (SJET)** is the modest effort to contribute and promote the research environment within the university and Pakistan as a whole. SJET is a peer-reviewed and multidisciplinary research journal to publish findings and results of the latest and innovative research in the fields. Following the tradition of Sukkur IBA University, SJET is also aimed at achieving international recognition and high impact research publication in the near future.

**Prof. Nisar Ahmed Siddiqui**
*Sitara-e-Imtiaz*
**Vice Chancellor**
**Sukkur IBA University**
Patron **SJET**

# Editorial

*Dear Readers,*

It is immense pleasure to present you the Third issue of Sukkur IBA Journal of Emerging Technologies (SJET). Sukkur IBA University firmly believes in research environment and has provided a platform for the intellectuals and researchers to share knowledge and new findings on emerging trends in various research areas to solve the difficult technical problems related to the technological advancements in response to the demands of the times. The SJET provided interdisciplinary platform to researchers' community to collaborate, co-innovate and instigate efforts to break the technological barriers. This journal provides the opportunity to gain and present authentic and insightful scientific & technological information on the latest advances in the field of emerging technologies.

The SJET provides invaluable source of information and enables the interested researchers to access the original information they are seeking. The manuscripts submitted in SJET have been followed by double-blind peer-review process, which addresses key issues in the field of emerging engineering technologies. The SJET has endorsed highly standards which are prerequisite for publishing high quality research work. This journal manifests into eco-system for the academician and engineers work together in the pursuit of excellence & innovation, that is why the editorial board of SJET is comprises of academic and industrial researchers from various advanced countries. The journal has adopted Open access policy without charging any publication fees that will certainly increase the readership by providing free access to a wider audience.

On behalf of the SJET, I welcome the submissions for upcoming issue (Volume-3, issue-1, January – June 2020) and looking forward to receive your valuable feedback.

I hope this journal will make a difference in our perspective and choice of research.

Sincerely,

**Dr. Saeed Ahmed Khan**
*Chief Editor*
**SJET**

===============================================================================
Publisher: **Sukkur IBA Journal of Emerging Technologies (SJET)**
**Office of Research, Innovation & Commercialization – ORIC**
**Sukkur IBA University** - Airport Road Sukkur-65200, Sindh Pakistan
Tel: (09271) 5644233 -37 Fax: (092 71) 5804425 Email: sjet@iba-suk.edu.pk URL: sjet.iba-suk.edu.pk
===============================================================================

# Contents

# A High State of Modular Transistor Design on A 105 Kw HVPS for X-Rays Tomography Applications

Hamayun Khan[1,4], Muhammad Yousaf Ali Khan[1], Qaisar Bashir[2] Amad ud din[3], Kashif Janjua[4] ,Shahid Khan[5]

**Abstract:**

 X-rays tomography work for the production of enhanced imaging at low radiation rate. This technique uses two tube of high voltage input power supply (HVPS) at different values, but such type of technique is so expensive. Another technique that have single tube of high voltage power supply have the ability to produce same high voltage at high rate of switching. This technique is so fast and less costly than the previous technique. In this paper, such type of high voltage input power supply (HVPS) technique is used. This technique consists of high state of modular transistor known is IGBT. The IGBT converts the applied power supply into high voltage power as input supply (HVPS) at the rate of 71 kHz, due to which the efficiency is increases to work for high values of load. This technique is tested for both resistive load and X-ray tube and their results are presented. This developed technique is also usable for other applications which are operated on high voltage power supply (HVPS). 3

*Keywords*: X-ray, high voltage power supply (HVPS)

## 1. Introduction

X-ray tomography works to radiate rays to obtain images of an object at different level of applied voltage. As we know x- rays have the ability to have different attenuation at the different level of energy. As a result, the images have more information about every parts of the object as compared to mano energy scan techniques. To replace dual scanning of an object the CT scanners were introduces of dual source. Now days this technology is so entrenched [1]. This technique consists of high voltage two tube for input power supply. One tube has high voltage typically 140 kV and the other have low voltage typically 80Kv, but unfortunately this technique is so costly another technique we want to introduce that have single tube of high voltage power supply having the ability to produce the same voltages as in the previous technique at high switching to change from voltage level to another, as result we can use multi-level of energy with one single tube.

---

[1] Department of Electrical Engineering, Gomal University, D.I.Khan, KPK, Pakistan

[2] Department of Electrical Engineering, University of Lahore, Lahore Punjab, Pakistan

[3] Department of Physics, Fatima Jinnah Women University, Rawalpindi, Pakistan

[4] Department of Electrical Engineering Superior University, Lahore, Punjab, Pakistan

[5] United Consulting Services, D.I.Khan, KPK,Pakistan

There are some basic ideas, e.g., in [2, 3]. The modulation in the range frequency will be 10-100 Hz depend on the uses and our need the switching from one level of energy to another is so fast typically less than 100-200 μs that generate quasi-rectangular pulses such type of technique gives excellent performance at low cost such technique in case of DC is known as a long-pulse HVPS. Generally, there are some devices which increase the size of the charging power but decrease the output efficiency. We need to overcome these types of challenges [4].

When the frequency is increased without the use of converter module as a result efficiency is going to decrease. In this paper we have to abolish this type of weakness and bring the developmental work for CT & DE. Heat control by using separate hardware architecture and bit-partitioning method is illustrated in [5]. The author considered an extra efficient mechanism by inducing newer memory chips for accessing register files. Bit-partitioned Register File (BPRF) from basic cache organization mechanism is considered. It is designed on a conventional dynamically scheduled superscalar processor [6, 7].

## 2. Main design parameters

High voltage power supply CT scan have major application in the field of medical which have maximum power of about 105 kW. Our major target is to bring down the size and also the cost. We have to make HVPS so strong that it can support the rotational force of typically 50 G. HVPS have two tube for power supply and also high-speed rotor for the rotation of anode.

The specifications are shown in Table 1, the expository part of the high voltage power supply technology is focused conversion from DC to DC. The HVPS has the flexibility and compatibility applications which are the main features.

## 3. HVPS design

The simplified block diagram is shown in below figure 1. The small size and low-cost capacitive filter are used in the AC chassis. The chassis filter, the large component of RL is at the HV side. An inductive adder is used for the conversion of DC to DC which consists of two module M1 and M2 which phase shifted the HF ripple suppression [8]. While satisfying the specification of HF ripple with the help of two circuit known as voltage multiplicative R1, R2. The high frequency switching circuit has low capacity typically of less than 200 pF. Due to this the converter is so nimble and useful for fast transition of low voltage state to high voltage state. As we know there are two inverter cells M1 and M2 as shown in below figure consisting of half-bridge inverters INV1, INV2. The zero-current switching (ZCS) mode, the inverter is operated in low line while at full load the inverter operates at 70kHz. In the other mode, the low frequency is observed. The IGBT is used which has less loss and low cost [11, 12].

**Table I:** Descriptions of HVPS for DE applications.

| | |
|---|---|
| Peak output power | 105 kW |
| Average power | 6 kW |
| Load voltage | -65 kV to -145 kV |
| Load voltage regulation | ±0.15% |
| High frequency (HF) ripple | <4% peak-to-peak |
| Low frequency (LF) ripple | <0.4%rms |
| Output Stored Energy | < 6 J |
| Load current | 12 mA to 930 mA |
| Conversion frequency | up to 60 kHz; |
| Input Voltage | 3 phase 400V AC |
| Typical cable capacitance | 200 pF |
| Dynamic Response: | slew rate >1 kV/us; |
| DE pulse repetition rate (PRR) | 10-1500 Hz |
| Depth of Modulation (DoM) | zero to 100% |
| Insulation (HV unit) | Solid |
| Lifetime | $5\times10^9$ shots at 50% DoM and $10^7$ shots at 100% DoM |
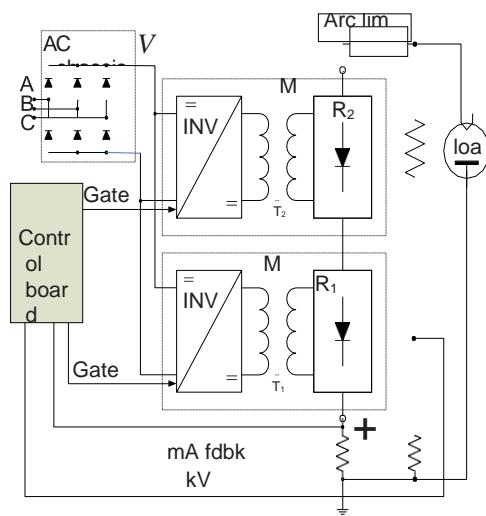
**Fig 1:** Block-diagram of HVPS.

The two transformers T1 and T2 are operated by eight inverters and each transformer have four inverters which are enabled and disabled according to the current operational condition. As the HV transformers have leakage inductance which consists of resonant tank circuits so there is no need of external inductors. The inverter consists of two chassis known as inverter chassis as shown in figure 2 and high voltage chassis as shown in figure 3. High voltage chassis provide insulation for hardness while inverter chassis have importance for the high rotational force of typically 50G. A lot of stress is observed on insulation and other parts during the pulse mood operation. We should need specific insulation system at DE pulse mode. The insulation design is best after testing obliges by FEA.



**Fig 2**: Inverter chassis having Weight of 37kg.



**Fig 3:** High voltage chassis consist of two transformers having secondary of 140kV.

The base of control section is FPGA which has standard features and so fast digital processing which consist of multiple protection like arc/spark, overheating of major component, over or under current and voltage and the interlock through current and voltage programing. In the frequency mode the inverters are active to regulate the output. When the load voltage in switching frequency increases for every period Ts, the PID control are not able to obtain the flat-top pulses in the wide range of input lines and loads which is changeable task in the case when line and load are fixed.

When the load voltage raises the inverter operates at Maximum frequency and as result

maximum power charging is obtained and reaches to the desired level. At this stage the converter is in feedback control and frequency is derived by this equation.

$$P_L = 4f_s C_r V_r^2$$

where

$P_L$ = Load Power

$f_s$ = Switching frequency

$C_r$ = Resonant frequency

$V_r$ = DC rail voltage

$$f_{ct} = \frac{P_L}{2*2C_r V_r^2}$$

(1)

We observed that PSpice model of HVPS is at full scale. All the features of HVPS are reproduced which are phase shifted in addition to the feedback loop.

## 4. Experimental results

Many HVPS are manufactured on compliance for specification. The wave form is obtained for resistive load and x-ray load are given below. Figure 4 is the wave form that is obtained for resistive load with high voltage switching in the range of -80kV to -135kV. The rise time is 100us at which power is high typically at 105kw for low load and decreases at high load. Figure 5a shows low line collector current at full power.

The Zero Current Switching (ZCS) remains the same and switching frequency reach to 70 kHz. At lower load and high load, the (ZCS) is also observed. Primary current which is phase shifted of the transformer T1, T2 having two inverters inside each module M1 and M2. At high load the collector current is indicated as shown in figure 5b. Due to non-ideal decoupling in each module some asymmetry is produce in the primary current.

When the test is started for the x-ray tube there should be measurable device to measure the external applied voltage so that we will be able to provide the needed voltage to the x-ray tube. If the external applied voltage is less than the needed voltage, then the feedback divider is used to increase the external applied voltage.
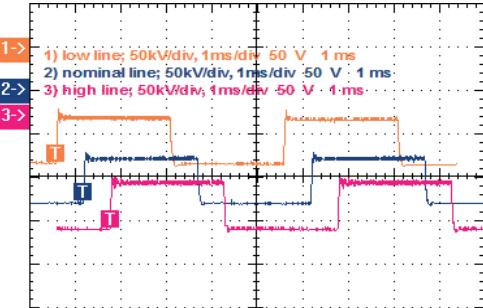


**Fig 4:** Resistive load= 181 kT.
High voltage= -135kV
Low voltage= -80kV
PRR=200 Hz.
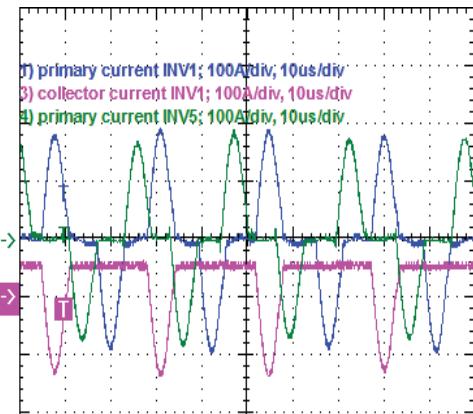


**Fig 5a:** low line collector current and full power.
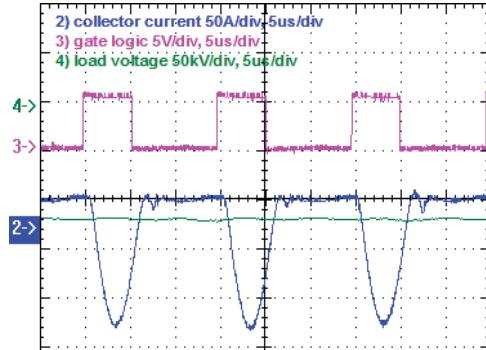
**Fig 5b:** Collector current due to non-ideal decoupling.
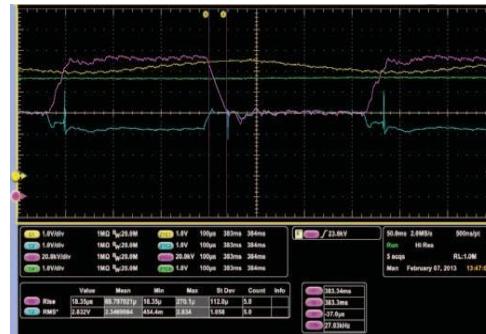


**Fig 6**: X-ray tube.

High voltage= -135kV
Low voltage= -80Kv
Load current= 533mA
PPR= 200Hz

To operate the x-ray tube efficiently, the maximum error is 1.5% due to the changing of the applied voltage after 200us. The wave form obtained during this operation are given in figure 6, and figure 7. When the frequency of the wave is increased from 1 kHz due to the rise and fall so that it takes another 100 usec to settle its efficient value. So, the average frequency for the implementation of this operation.
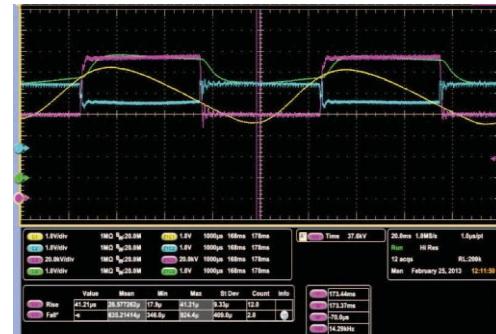


**Fig 7:** X-ray tube

High voltage= -135kV
Low voltage= -80Kv
Load current= 533mA
PPR= 1500Hz
Rise- and fall time= 40 μs.

The heat control by using separate hardware architecture and bit-partitioning method is illustrated in [1]. The author considered an extra efficient mechanism by inducing newer memory chips for accessing register files. Bit-partitioned Register File (BPRF) considered their designing mechanism from basic cache organization mechanism. It is designed based on a conventional dynamically scheduled superscalar processor. When test for the resistive load is started, the operation duration is from 15 sec to 100 sec at power of 36 kW. All the components are also reliable. After some time, all the IGBT in the inverters have base plate start to become overheat due to which the voltage drops increase the temperature produce in such a case are 37ºC which is the worst case.

## 5. Conclusion

In this paper a HVPS is developed which have high performance and low cost which is tested for both resistive load and also for the

x-ray tube. By using this technique, we are able to produce 105kW to 140KW power at the frequency rate of 1.5 kHz by using single tube.

# REFERENCES

[1] M. P. Musau, N. A. Odero, and C. W. Wekesa. "Asynchronous interconnection of the proposed East Africa Power Pool (EAPP)," 2017 IEEE PES Power Africa, June 2017, pp. 7-11.

[2] C. Chen, K. Zhang, K. Yuan, Z. Gao, X. Teng, and Q. Ding. "Disturbance rejection-based LFC for multi-area parallel interconnected AC/DC system," IET Generation, Transmission & Distribution, vol. 10, No. 16, pp. 4105-4117, Dec. 2016

[3] X. Zheng, Y. Chen, H. Chen, Y. Zhang, J. Zhu, J. Chen, and P. Xuan. "Loss-Minimizing Generation Unit and Tie-Line Scheduling for Asynchronous Interconnection," IEEE Journal of Emerging and Selected Topics in Power Electronics, to be published, DOI: 10.1109/JESTPE.2017.2783930

[5] H. Khan, M. U. Hashmi, Z. Khan, and R. Ahmad, "Offline Earliest Deadline first Scheduling based Technique for Optimization of Energy using STORM in Homogeneous Multi- core Systems," IJCSNS Int. J. Comput. Sci. Netw. Secur. VOL.18 No.12, December 2018, vol. 18, no. 12, pp. 125–130, 2018.

[6] H.E. Daniels et al., "Dual Voltage X-Ray Switching System", European Patent 052 269, 1985.

[7] B. M. Gordon et al., "Dual Energy Power Supply", US Patent 5,661,774, Aug. 26, 1997.

[8] H. Khan, M. U. Hashmi, Z. Khan, R. Ahmad, and A. Saleem, "Performance Evaluation for Secure DES-Algorithm Based Authentication & Counter Measures for Internet Mobile Host Protocol," IJCSNS Int. J. Comput. Sci. Netw. Secur. VOL.18 No.12, December 2018, vol. 18, no. 12, pp. 181–185, 2018

[9] C. Loef and G. Zeitler, "Power Supply for an X-Ray Generator System Comprising Cascade of Two Voltage Sources", European Patent EP 2 207 405 B1, 2013.

[10] A. Pokryvailo, C. Carp, and C. Scapellati, "A High-Power High Voltage Power Supply for Long-Pulse Applications", IEEE Transactions on Plasma Science, Vol. 38, No. 10, October 2010, pp. 2604-2610.

[11] A. Pokryvailo, C. Carp, and C. Scapellati, "High Power, High Performance, Low Cost Capacitor Charger Concept and Implementation", IEEE Transactions on Plasma Science, Vol. 38, No. 10, October 2010, pp. 2734-2745.

[12] A. Pokryvailo, C. Carp and C. Scapellati, "Highly Efficient Switch- Mode 100-kV, 100-kW Power Supply for ESP Applications", Proc. 11th Int. Conf. on Electrostatic Precipitation, Hangzhou, 21-24 Oct., 2008, pp. 284-288

# Analysis of Basic Spatial Gait Parameters in Laboratory

Shehla Inam[1] and Muhammad Waqar[2]

**Abstract:**

Human gait is performed by the locomotion of the lower limbs. The basic spatial parameters of gait cycle were measured in laboratory for the young healthy subjects including 13 females and one male in two conditions i.e. barefoot (assuming healthy gait) and wearing only one shoe (assuming unhealthy or compensated gait). The comparison between the two conditions was studied for the average values of step length, stride length, base of support and step width. Also, the standard deviation and coefficient of variance were calculated individually for each parameter of healthy subjects. The average values of the initial three parameters were greater for the healthy subjects while the fourth parameter calculated was greater for the unhealthy subjects.

**Keywords:** *Basic gait parameters; gait analysis; spatial gait parameters; gait laboratory studies*

## 1. Introduction

A gait cycle is the time period during which one of the legs is initially in contact with ground and after going through seven events of locomotion starting with initial contact, comes back to its initial position [3]. The gait analysis of a patient could help in revealing certain biomechanical problems which could be cured either through medical equipment, physical therapy or surgery. Also, this includes the neural and muscles pain [12] Rehabilitation plays and important role in coping up the injuries that are encountered in sports. Rehabilitation process involves certain steps designed in [2]. Tommy Oberg et.al studied the basic gait parameters of 233 subjects in a 5.5 m long gait laboratory including both men and women. The parameters were measured for the slow, medium and fast gait. They found the significant age-variability in walking speed and step length for normal and fast gait and the effect of age and sex for normal and fast gait [1]. M.M. Samson et.al investigated the effects of age, weight and height on the normal walking speed of the healthy subjects including both men and women. They used certain devices such as Kistler force plates for cadence measurement, an infrared reflecting system for measuring the walking speed and the stride length via the formula. They concluded that cadence did not depend upon the age, weight and height while the stride length and walking speed reduced with the age [4]. Emily A. Ready et.al investigated the effects of auditory cues on the gait of healthy

---

[1] Department of Biomedical Engineering, Riphah International University, Islamabad, Pakistan

[2] Department of Biomedical Engineering and Sciences, National University of Sciences and Technology Islamabad, Pakistan

*Corresponding Author: shehlainam10@gmail.com

subjects depending on their ability of beat perception while following certain conditions. Thus, the spatiotemporal gait parameters were influenced when walking to music- and metronome-based rhythmic auditory stimuli [5]. In [6], the relationship between two gait parameters i.e. in-laboratory gait speed measured through pressure sensor of a sheet-type and daily gait speed via accelometer was investigated among the older subjects. The relationship between both parameters was found out to be low, However, the average daily gait speed was significantly lower than average in-laboratory gait speed. Claudiane A.Fukuchi and MarcosDuarte proposed a simple method to predict the gait pattern of the subjects based on their speed by creating a reference database consisting a range of gait speeds and predicted database for gait pattern. Thus, the predicted data was the same compared with the experimental measures for the joint angles and joint moments [7]. Pierre Martz et.al assessed the influence of body mass index on the gait parameters of the patients including both obese and non-obese patients suffering from total hip anthroplasty before and after the six months of surgery. The patients had shown a significant functional improvement regardless of BMI [8]. Roth et.al studied the relationship between the spatial parameter i.e. speed of walk and the 18 temporal parameters among the patients of one-month hemiplegia. The experiment was performed with the help of footswitches connected to portable device. The speed was found to be corelated with most but not all the temporal parameters [9]. In [10], the authors studied the difference in the biomechanic parameters among the healthy and the moderate and chronic osteoarthritis patients. They concluded that the knee osteoarthritis patients showed results such as lower knee and ankle joint moments, ground reaction forces, knee reaction force and knee excursion on desired speed. There was decreased knee joint excursion for all conditions during analytic differences in walking speed. M.Ambrus et.al analyzed the difference in the stride length-cadence relationship among fifteen patients of Parkinson's disease and fifteen age-matched subjects both on treadmill

and overground through linear regression. It was observed that the treadmill had positive impact on the gait of patients of Parkinson's disease [13]. The differences in kinetic and kinematic were studied during the landing mechanics of a single leg drop jump between an athlete suffering from no ACL injury history in their past and an athlete who suffered from the ACL reconstruction surgery. The latter had low range of their hip, ankle and knee motion in two planes i.e. sagittal and frontal during a single drop jump and had relatively higher ground reaction forces [14].
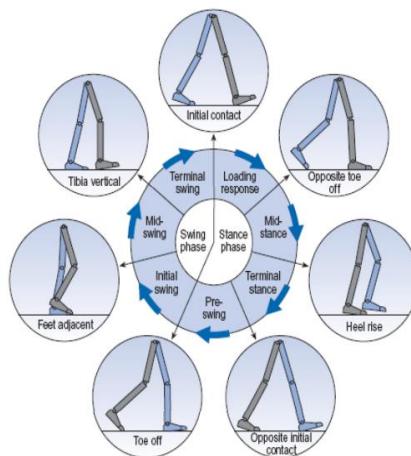


**Fig. 1** Seven Events of Gait Cycle

## 2. Methodology

### 2.1. Subjects Recruitment

The seven parameters of gait of 14 subjects including 13 females and one male of age (21.38±1.64), weight (56.57 ±10.03) and height (64.92″±3.53) were measured and studied. The experiment was performed with the consent of subjects in the laboratory of Department of Biomedical Engineering, Riphah International University, Islamabad.

### 2.2. Measurement of Parameters

The parameters that were measured included step length, step width, stride length, base of support, stride length/ length of lower extremity and cadence. The study was undertaken in such a way that the subjects were asked first to perform the gait barefoot.

This was assumed as a healthy gait. Next, they were asked to perform an unhealthy or compensated gait. This was done by wearing one shoe in one foot and the other left barefoot. This gave an expression of a compensated gait because of the difference in the height of both feet and also the change in their gait was observed. All the desired parameters were measured with the help of a long scale of 100 centimeters and a stop watch was used to calculate the cadence. In cases, where the measurements exceeded 100 centimeters, a point was marked, and the measurements were added by putting the scale on the marked point and re-measuring from the initial value of the scale i.e. 1 centimeter. The comparison between the assumed healthy and unhealthy subjects was studied only for four parameters i.e. step length, stride length, base of support or walking base and step width. After measuring each parameter of all the subjects, the average, standard deviation (St.Dev.), and coefficient of variance (CV) for each parameter were calculated as shown in table II.

**Table I:** Gender information of each subject

| Sr.No. | Gender | Age | Height | Weight | Dominant Leg | History of Injury | If flat foot | Family History |
|---|---|---|---|---|---|---|---|---|
| 1 | female | 22 | 5'3" | 53 | right | no | no | diabetic |
| 2 | female | 22 | 6.0' | 70 | right | no | yes | diabetic |
| 3 | female | 22 | 5'8" | 49 | left | no | no | no |
| 4 | female | 22 | 5'3" | 58 | right | no | yes | diabetic |
| 5 | female | 22 | 5'3" | 56 | right | no | no | diabetic |
| 6 | female | 21 | 5'2" | 46 | right | no | no | no |
| 7 | female | 21 | 5'3" | 72 | left | no | no | diabetic |
| 8 | female | 22 | 5'7" | 50 | right | no | no | no |
| 9 | female | 21 | 5'3" | 80 | right | no | no | no |
| 10 | female | 23 | 5'5" | 50 | right | no | no | no |
| 11 | female | 24 | 5.2' | 60 | right | no | no | no |
| 12 | female | 23 | 5'0" | 50 | right | no | no | no |
| 13 | female | 18 | 5'6" | 48 | right | no | no | no |
| 14 | male | 18 | 6.0' | 50 | right | no | no | diabetic |

### 2.3. Gender Information

Before carrying out experiment, the basic information including the gender, height, weight, dominant leg, history of injury, flat footness and family history of each subject was recorded as shown in table I.

## 3. Results and Discussion

The parameters for the healthy gait of the subjects that were measured are shown in table II.

**Table II:** Measured parameters of healthy subjects

| Sr.No. | Step L (cm) | Stride L (cm) | BOS (cm) | Step W (cm) | Cadence (steps/min) | SL/LEL | Speed (cm/s) |
|---|---|---|---|---|---|---|---|
| 1 | 58.2 | 85 | 22.5 | 8 | 82 | 0.6 | 79.5 |
| 2 | 62.1 | 96.2 | 24.75 | 14.5 | 35 | 0.96 | 36.2 |
| 3 | 59.9 | 92.5 | 22.5 | 5.6 | 76 | 0.94 | 75.8 |
| 4 | 40.6 | 86.3 | 23.8 | 4.8 | 105 | 0.9 | 71.1 |
| 5 | 39.5 | 82.3 | 24.9 | 3.3 | 101 | 0.83 | 66.5 |
| 6 | 36.1 | 80.8 | 22.4 | 2.54 | 114 | 2.3 | 68.6 |
| 7 | 48.4 | 121.9 | 23.4 | 5.08 | 273 | 3.12 | 220.2 |
| 8 | 59.7 | 120.6 | 23.1 | 2.54 | 240 | 3.12 | 238.8 |
| 9 | 51.3 | 107.4 | 24.1 | 3.81 | 20 | 0.6 | 17.1 |
| 10 | 12 | 45 | 22.1 | 8.5 | 38 | 0.48 | 7.6 |
| 11 | 16 | 78 | 26.1 | 5.5 | 108 | 0.85 | 28.8 |
| 12 | 41 | 81 | 24.5 | 10 | 78 | 0.96 | 53.3 |
| 13 | 52 | 89 | 23 | 15 | 70 | 0.76 | 60.7 |
| 14 | 74.5 | 137.5 | 22.8 | 25 | 110 | 1.50 | 136.6 |
| Average | 46.5 | 93.1 | 23.6 | 8.2 | 103.6 | 1.2 | 46.5 |
| St.Dev | 17.4 | 23.0 | 1.2 | 6.3 | 71.5 | 0.9 | 17.4 |
| CV | 37.3 | 24.7 | 5.0 | 77.1 | 69.1 | 73.6 | 37.3 |

Likewise, the parameters for the unhealthy gait that were measured are shown in table III.

### 3.1. Step Length

The step length is the distance covered by one right and left leg as shown in Fig. 2. The subjects were asked to only take a step and stand on the same position. Initially, the value was measured by standing barefoot. Next, each subject was asked to wear a shoe only in one foot and the other foot bare which depicted as the compensated or unhealthy gait. Hence, in both cases, the values were measured with the help of a long scale in centimeters from the heel of trailing foot to

the heel of leading foot. The average of the values obtained is shown in Fig.3

**Table III**: Measured parameters of unhealthy subjects

| Sr.No. | Step L (cm) | Stride L (cm) | BOS (cm) | Step W (cm) |
|--------|-------------|---------------|----------|-------------|
| 1 | 34.6 | 76.4 | 23 | 13.9 |
| 2 | 60 | 118.5 | 25.5 | 15 |
| 3 | 64.5 | 82.5 | 23 | 9.5 |
| 4 | 41 | 87 | 24.2 | 5.1 |
| 5 | 41.3 | 83 | 25.5 | 4 |
| 6 | 44.4 | 93.9 | 2.6 | 5.6 |
| 7 | 56.1 | 117.1 | 25.6 | 4.8 |
| 8 | 56.9 | 119.3 | 23.1 | 2.5 |
| 9 | 48.3 | 104.1 | 24.1 | 3.2 |
| 10 | 9.8 | 19.5 | 12 | 19 |
| 11 | 35 | 69.5 | 22.5 | 9.2 |
| 12 | 36 | 97 | 26.6 | 12 |
| 13 | 47 | 67 | 23.2 | 12 |
| 14 | 56 | 130 | 23 | 24 |
| Average | 45.1 | 90.3 | 21.7 | 10.0 |
| St.Dev | 14.0 | 28.4 | 6.5 | 6.4 |
| CV | 31.2 | 31.4 | 29.9 | 64.2 |

.
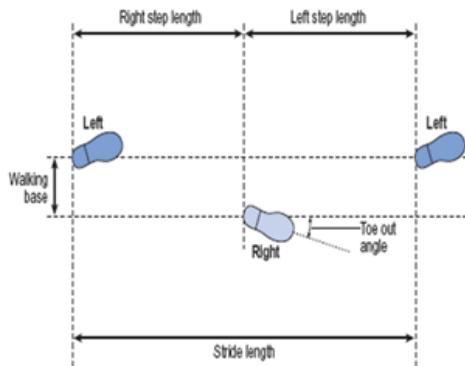


**Fig. 2**: Walking base (BOS), Step Length and Stride Length [3]

The Fig. 3 shows that the step length of the healthy subjects i.e. having worn no shoes had a greater step length as compared to those wearing only one shoe. This could be because the muscles of the healthy subjects were more active and felt no hindrance in performing the step because of greater stability. However, the unhealthy subjects did require taking relatively smaller steps to not losing their balance.
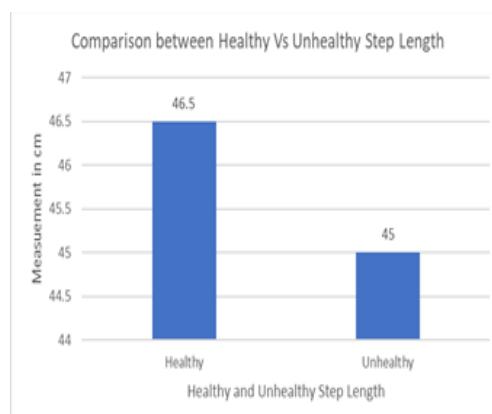


**Fig 3:** Healthy Vs Unhealthy Step Length

### 3.2. Stride Length

The stride length is the distance covered by two consecutive steps as shown in Figure 3. Each subject was asked to firstly, take steps barefoot and next time, take steps while wearing only one shoe. Thus, the values were measured with the help of a long scale in centimeters by measuring the distance from the heel of the already heading foot when one step was taken previously, and to the heel of the foot which was brought ahead of it to take another step. The average of the values is shown in Fig. 4.
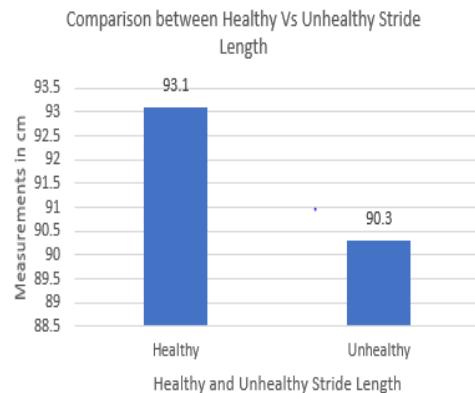


**Fig 4:** Healthy Vs Unhealthy Stride Length

From Figure 4, it can be observed that the stride length of the healthy subjects was

greater as compared to that of unhealthy subjects due to covering a large distance and taking longer steps. Their muscles had more control in maintaining stability and performing stable steps.

### 3.3. Base of Support or Walking Base

The base of support as shown in Figure 2 is actually the area covered by the whole length of the foot. Hence, it was measured by measuring the length of the foot with the help of a scale in centimeters by placing both the feet still. The average of the values of the base of support obtained for both cases i.e. healthy (barefoot) and unhealthy (one foot with shoe) is shown in Fig. 5.

Fig. 5 shows that the base of the support for the unhealthy subjects is smaller than those of healthy subjects. It may be because the subjects with abnormal gait require greater stability to stand on their feet as compared to those with a normal gait.
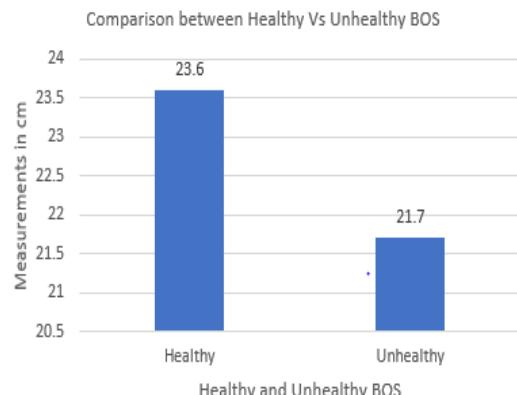


**Fig 5:** Healthy Vs Unhealthy Walking Base

### 3.4. Step Width

The step width as shown in Figure 6 is the horizontal distance between the two feet while taking a step. Thus, it was measured by measuring the distance horizontally from the heel of the leading foot to heel of the trailing foot in both cases i.e. healthy and unhealthy gait. The Figure 7 shows the average values of the step width for both cases.
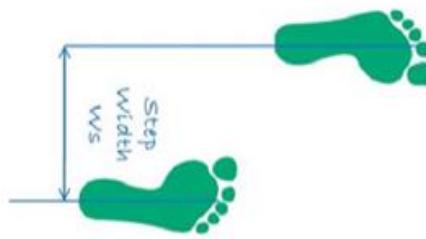


**Fig 6:** Step Width [11]



**Fig 7:** Healthy Vs Unhealthy Step Width

It can be observed from the Figure 7 that the average value of step width of unhealthy subjects is relatively greater than those of healthy subjects. This may be because they require greater step width to increase their balance and stability.

However, the other parameters i.e. cadence, and the ratio stride length/ lower extremity were not measured for the unhealthy condition of the subjects.

### 3.5. Cadence

Cadence is the number of steps taken in one minute. Thus, the healthy subjects were asked to perform the gait barefoot in their normal speed in one minute. The values were recorded with the help of a stop watch which are shown in table II. However, cadence of the unhealthy subjects was not calculated.

### 3.6. Stride Length/ Lower Extremity Length (SL/LEL)

The lower extremity's length was measured by tape measurement from greater trochanter to lateral maleollus. Thus, the ratio of SL/LEL was calculated for the healthy gaited subjects as shown in table II. The average value calculated is 1.2±0.9.

### 3.7. Speed

The walking speed of the healthy or barefoot gait of the subjects was measured by formula,

*Speed= Step Length\* Cadence*

The values calculated for the speed could be observed in table II. The average value for the speed of healthy gaited subjects calculated is 46.5±17.4.

## 4. Conclusion

The basic gait parameters play a vital role in the overall gait performance of a person. Thus, an experiment was carried out to study the basic spatial parameters of the healthy subjects in two conditions i.e. once barefooted and next wearing only one shoe assuming it as compensated gait. The parameters such as step length, stride length and base of support of the healthy gaited subjects were greater as compared to that of unhealthy gaited subjects. However, the step width of the unhealthy gaited subjects was greater. Moreover, the other parameters i.e. cadence, SL/LEL and speed were measured only for the healthy subjects. The studies on these parameters for the compensated gait could play a vital role in the future research.

**REFERENCES**

[1] A. K. a. K. O. Tommy Oberg, "Basic gait parameters: Reference data for normal subjects,," Journal of Rehabilitation Research, pp. 210-223, 1993.

[2] K. JG, "Introduction to Rehabilitation," Clinics in Sports Medicine, 2010.

[3] V. S. J. S. D. Ashutosh Kharb, "A review of gait cycle and its parameters," in IJCEM International Journal of Computational Engineering & Management, 2011.

[4] A. C. L. d. V. A. G. D. A. D. J. J. V. M. M. Samson, "Differences in gait parameters at a preferred walking speed in healthy subjects due to age, height and body weight," Aging Clinical and Experimental Research, vol. 13, no. 1, pp. 16-21, 2001.

[5] E. A. et.al, "Beat perception ability and instructions to synchronize influence gait when walking to music-based auditory cues," Elsevier, vol. 68, pp. 555-561, 2019.

[6] N. T. et.al, "Relationship between Daily and In-laboratory Gait Speed among Healthy Community-dwelling Older Adults," Scientific Reports, 2019.

[7] C. A. a. MarcosDuarte, "A prediction method of speed-dependent walking patterns for healthy individuals," Elsevier, vol. 68, pp. 280-284, 2019.

[8] P. M. et.al, "Influence of body mass index on sagittal hip range of motion and gait speed recovery six months after total hip arthroplasty," International Orthopaedics, 2019.

[9] R. et.al, "HEMIPLEGIC GAIT: Relationships Between Walking Speed and Other Temporal Parameters1," American Journal of Physical Medicine & Rehabilitation, vol. 76, no. 2, pp. 128-133, 1997.

[10] [10] J. A. Z. J. a. J. S.Higginsonb, "Differences in gait parameters between healthy subjects and persons with moderate and severe knee osteoarthritis: A result of altered walking speed?," Elsevier, vol. 24, no. 4, pp. 372-378, 2009.

[11] P. A. a. B. Mullarney, "The relationship between pedestrian loading and dynamic response of an FRP composite footbridge," Bridge Structures, 2018.

[12] A. C. Lee, "CHAPTER 5: Physiologic and Pathologic Gait," in Principles and Practice of Pain Medicine.

[13] J. a. M.-d.-O. M.Ambrus, "Walking on a treadmill improves the stride length-cadence relationship in individuals with Parkinson's disease," Gait and Posture, vol. 68, pp. 136-140, 2019.

# Bio Methane from Biogas, Renewable Energy Resource for Pakistan

Asif Ali[1]

**Abstract:**

The major barriers in development of Pakistan's economy are dependency on inefficient and unaffordable energy technologies, thus it is an energy-short country. The future energy demands of the country can be fulfilled by opting renewable energy technologies. The number of biogas energy generation Systems is increasing steadily, as they are generated with low-cost. Pakistan's 70% population is residing in rural areas, so biogas energy can be a good substitute. A national policy regarding the development of biogas energy technology is needed to enhance the biogas potential. This study focuses on control of agriculture waste by chemical absorption process, in which the biomass is converted into fuel. In this way not only, biomass is treated but renewable energy can be generated. The raw material, biomass, was fed to an anaerobic digester that operates at 35° and produces biogas along with sludge biomass. The mixture of biogas and sludge biomass was separated with the help of flash unit and further separation was done by centrifuge to get concentrated biomass and water. The raw biogas was compress from 1 bar to 5 bars in order to remove ammonia from biogas. The biogas was upgraded to bio methane in an absorption column by treating biogas with potassium hydroxide. The biomass potential of Pakistan which is 853,500 tons/day can be utilized by using this process to generate 469,425 tons/day of bio methane. Cost analysis indicated that the chemical absorption is feasible.

**Keywords**: *Biogas, Hydrogen sulfide, Chemical absorption, Potassium hydroxide, Bio methane, Renewable energy*.

## 1. Introduction

### 1.1. Energy Situation in Pakistan

Pakistan is facing energy crises, major energy resources are oil and gas, the country's reserves of oil and gas are finite and hence oil is imported on a very large scale. The oil imported, covered approximately 31% of the country's energy necessity. The oil import bill of Pakistan increasing year by year, from it was about $7 billion and increase to $12 billion in 2011.

The conventional energy sources provide more than 99% of the energy and only 1% energy supply is from renewable sources. For the year 2010-2011, aggregate energy consumption was 38.8 million tons of oil, of which 38.5% was used up by the industrial sector, 30.9% was consumed by transport, and agriculture only used 2% of the total intake. [1]

[1] Department of Renewable Energy Engineering, USPCAS-E, Peshawar
*Corresponding Author: chemasif85@gmail.com

## 1.2. Renewable Energy

Renewable Energy is described as the form of energy which resources are naturally and can be replaced on a human timescale. The conventional (non-renewable) sources of energy are depleting at a faster rate day by day and this drawback is leading to move towards the renewable energy. Renewable energy has a vast potential to cover our future energy demands and overcome worldwide energy crisis. The natural resources of renewable energy include; wind, biogas, tides, rain, geothermal heat and sunlight, etc.

Availability of renewable energy resources over wide geographical regions differentiate it from other conventional energy sources, which are limited to a few countries.

Another main advantage of using renewable resources is that, air pollution caused by burning of fossil fuels, can be controlled and develops public health by reducing sickness ratio caused by pollution and save linked health costs. [2]
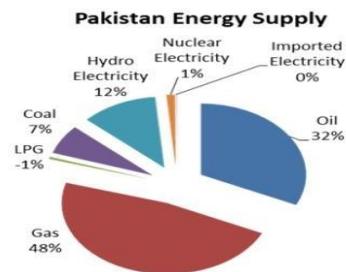


**Fig 1:** Pakistan Energy Supply by source
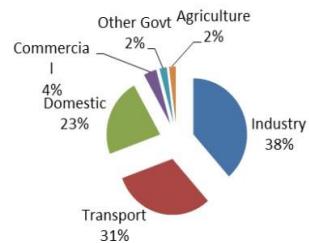


**Fig 2:** Pakistan Energy Consumption by sector

## 1.3. Biogas

A blend of various gases collected by the disintigration of organic matter in the absence of oxygen is known as biogas. Agriculture waste, municipal waste, plant material, sewage, food waste, and animal waste etc. are the raw materials from which biogas can be extracted.

The biogas composition is mostly composed of methane (CH4) and carbon dioxide ($CO_2$) and addition to this, insignificant quantity of hydrogen sulfide ($H_2S$), moisture and siloxanes may have also present in the biogas. The methane, and other gases, hydrogen, and carbon monoxide can be combusted or oxidized with oxygen. This energy release upon combustion let biogas to be used as:

- Fuel
- Heating purposes
- Gas engines [3]

The waste can be treated by several processes:

- Open air windrow composting
- Incineration
- Landfill
- Mechanical biological treatment
- In-vessel composting
- Anaerobic digestion. [4]

**Table I**: Composition of Biogas

| Gases | Percentage % |
|---|---|
| Methane | 50 – 75 |
| Carbon dioxide | 25 – 40 |
| Nitrogen | 0 – 10 |
| Hydrogen | 0 – 1 |
| Hydrogen sulfide | 0 – 3 |
| Oxygen | 0– 2 |

## 1.4. History of Biogas in Pakistan

The history of biogas in Pakistan is almost fifty-nine years old. In 1969, the first farmyard manure plant was buildup in Sindh to produce biogas from animal and farm waste. The Government of Pakistan inaugurated total

4,140 biogas plants under a comprehensive biogas scheme in 1974 up-to 1987. In 1982 to 1985, one thousand biogas plants were installed in several districts of Punjab. Another seven hundred and fifty family size biogas plants were installed all over Punjab as a scheme a program 'Adaptation of biogas technology to mitigate the energy crises' of agriculture department in 2009-2010. [5]

## 1.5. Biogas Potential in Pakistan

Biogas may be beneficial to overcome the present energy disaster in Pakistan and its cost is 35 to 50 percent less than that of other energy resources like, charcoal, kerosene oil and firewood. Nowadays a big problem in Pakistan is energy crises and it could be handled by enriching livestock and dairy development. Animal dung can be utilized for the production of gas and a high-quality fertilizer as a byproduct. Pakistan has approximately 29.9 million buffalos, 33 million cattle. One buffalo or cow produces 15 kg dung per day and there are 56,900,000 animals and if 50 percent of this dung is collected, then 426,750,000 kg of dung every day is available for the conversion to biogas. A biogas plant can install within Rupees 40,000 to Rupees 150,000 and its components are easily attainable in the local market. [6]

## 1.6. Bio Methane

The upgraded form of biogas by removing traces like, hydrogen sulfide, carbon dioxide and moisture is known as bio methane. Biogas is the product of anaerobic digestion of raw materials like dead plant material, manure, sewage, organic waste, etc.
Although its usability is recognized for fairly some time, bio methane might be used as a possible source of energy, specifically for fossil fuels. Installation of plants for the producing of bio methane is new and initiated only in the recent years as an end result of the mounting prices of natural gas and high electricity prices. Bio methane and fossil fuel derived methane has a great difference between each other even though the certainty that both are originated from organic matter, and are same chemically.

The source of fossil fuel derived methane is old fossil residue of organic matter that lies buried deep in the ground from thousands or millions of years. While for the bio methane resources are "fresh" organic matter, available everywhere worldwide which marks it a renewable source of energy. [7]

## 1.7. Different Technologies for Upgrading Biogas to Bio Methane

### 1.7.1 Water and Polyethylene Glycol Scrubbing

As carbon dioxide and hydrogen sulfide are more soluble in water than methane, water scrubbing is used to draw out these traces from biogas. In this method, traces are absorbed in a counter-current operation. First, the biogas is pressurized and then fed to a packed column from the bottom while at top, water is fed.

The water contaminated very quickly when high levels of hydrogen sulfide are to be treated which cause operational problem, thus stripping with it is not recommended. [8]

### 1.7.2 Pressure Swing Adsorption

In this method, few gas species are separated from a mixture of gases under pressure cohering to the specie's molecular characteristics and affinity for an adsorbent material. Special adsorptive materials (e.g. zeolites and active carbon) are utilized as a molecular sieve, which adsorb the intent gas species at high pressure.

An additional step is needed before PSA for the elimination of hydrogen sulfide, which is the main disadvantage of PSA technology. [9]

### 1.7.3. Cryogenic Separation

Carbon dioxide, hydrogen sulfide and all other biogas traces can be sort out from $CH_4$ as each contaminant has specific temperature and pressure at which it liquefies. This segregation process requires low temperatures, near -100 ℃, and high pressures, almost 40 bars.

The requirement of substantial process equipment, such as compressors, turbines and heat exchangers are the main disadvantage of this process. [10]

### 1.7.4. Membrane Separation

In membrane separation the raw gas is passed through a thin membrane, some constituents are filtered out while the remaining components of the raw gas are accumulated at the surface of thin membrane. A ratio between high methane purity and high methane yield in the customized gas is created.

Relatively low methane yield and high membrane cost are the disadvantages of the membrane separation. [11]



**Fig 3:** Chemical Absorption Method

## 2. Methodology

Several researchers have worked on the different techniques used for the customization of biogas to bio methane. Some of these methods are already discussed in the introduction section. According to literature review the feasible, economical, and environmentally friendly technique is chemical absorption. Availability of several absorbents, like KOH, NaOH, and MEA used in this process is another advantage of chemical absorption. According to Grazia Leonzio, among these absorbents KOH is the suitable one, having low price and less environmental impact. [12]

### 2.1. Chemical Absorption

Reversible chemical bonds are developed between the solute and the solvent in chemical absorption. Therefore, with a high energy input, regeneration of the solvent includes splitting of these bonds. Chemical solvents are normally either aqueous solutions of amines (i.e. mono-, di-, or tri- ethanol amine) or aqueous solution of alkaline salts (i.e. sodium, potassium and calcium hydroxides).

Almost complete removal of hydrogen sulfide is one of the major advantages of chemical absorption, also high efficiency and tendency to operate at low pressure are considerable advantages of chemical absorption. This process is generally used in industrial applications, and many other applications, such as natural gas purification. [13]

### 2.2. Potassium Hydroxide (KOH)

The absorbent used in this process is potassium hydroxide, generally called caustic potash which is an inorganic compound. Due to its reactivity toward acids it has many industrial applications, most of which accomplishing its corrosive nature. KOH is remarkable as the precursor to most soft and liquid soaps as well as several chemicals which contain potassium. [14]

### 2.3. Overall process flow diagram

The raw material, agriculture waste as biomass, and water was fed to an anaerobic digester that operates at 35 ºC and produces biogas along with sludge biomass. The mixture of biogas and sludge biomass was separated with the help of flash unit and further separation was done by centrifuge to get concentrated biomass and water. The raw biogas from the flash unit was compress from 1 bar to 5 bars in order to remove ammonia from biogas. The biogas was upgraded to bio methane in an absorption column by treating biogas with potassium hydroxide.

**Fig 4:** Overall Process Flow Diagram

100 tons/day of biomass and 70% conversion of biomass is taken as basis. Material and energy balances are applied on each unit by considering the following assumptions:

- Mostly Theoretical based
- Steady state Process
- $\Delta w = \Delta K.E = \Delta P.E = 0$
- 98% Flash separation efficiency
- 80% centrifuge efficiency

For material balance the following equation is used:

Input + Generation = Output + Accumulation + Consumption
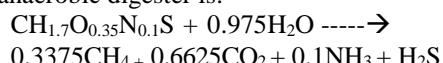
For energy balance the following equation is used:

$$Q = \sum m_{i,\,out} \times \Delta \hat{H}_{i,out} - \sum m_{i,in} \times \Delta \hat{H}_{i,in}$$

Physical data such as different specific heat capacities used in the stoichiometric calculations is taken from 'Elementary Principles of Chemical Processes by Richard M. Feldar'[15], while Thermodynamic data such as different enthalpies, from 'Fundamentals of Thermodynamics by Michael J. Moran & Howard N. Shapiro'[16]

The main reaction occurring in the anaerobic digester is:

$CH_{1.7}O_{0.35}N_{0.1}S + 0.975H_2O$ ----->
$0.3375CH_4 + 0.6625CO_2 + 0.1NH_3 + H_2S$

## 2.4. Individual Equipment Design

Length, diameter and volume for each equipment are calculated by using residual time and L/D ratio from literature, specific for each unit. For example, for the anaerobic digester:

Residual Time = 10 days
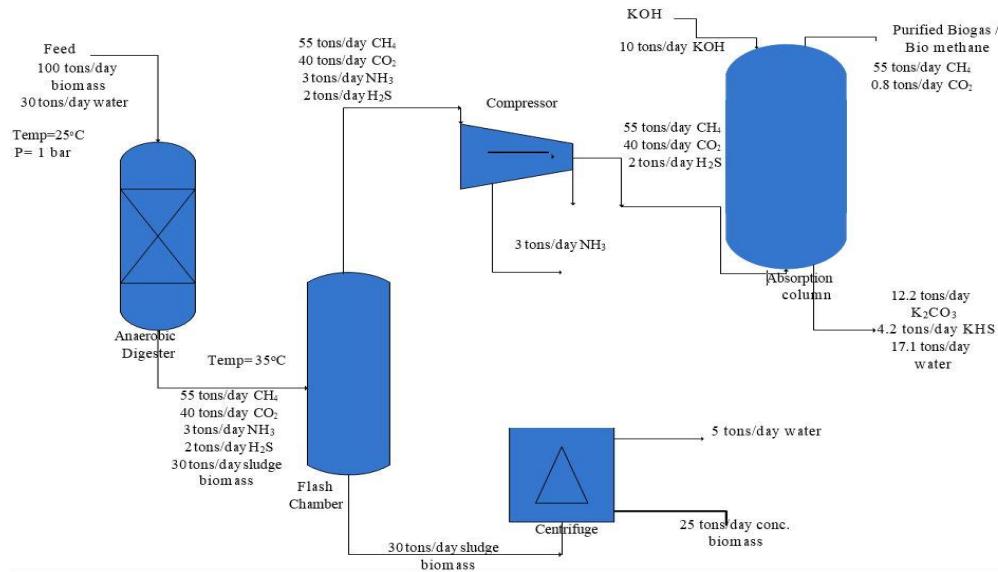
$$L/D = 1.7 \ [17]$$

Volume= Residual Time x Volumetric Flow Rate

## 2.5. Cost Estimation

Cost is calculated for each unit by using the following formulas, and the cost is estimated for the whole process to calculate the payback period of the unit.

- $C_{E,1} = C_B (Q / Q_B)^M$

**Fig 5:** Overall Process Flow Diagram with Material Balance

- $C_{E,1} / C_{E,2}$ = Index 1 / Index 2
- Total Equipment Cost (TEC) = $C_{E,2}$ $f_M f_P f_T$

$C_F = \sum_i f_M f_P f_T (1 + f_{PIP}) C_E + (f_{ER} + f_{INST} + f_{ELEC} + f_{UTIL} + f_{OS} +$

$f_{BUILD} + f_{SP} + f_{DEC} + f_{CONT} + f_{WS}) \sum_i CE$ [18]

## 3. Results

### 3.1. Bio Methane
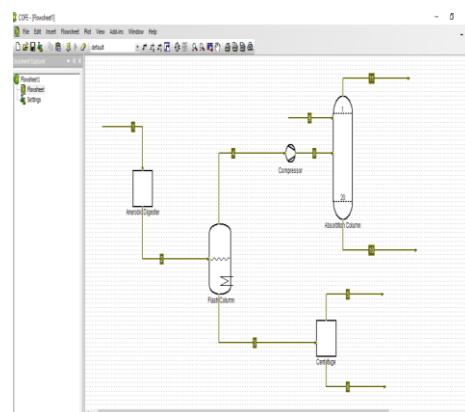
We have developed this process for an industrial scale and cannot use this process in laboratory because of the unavailability of such kind of equipment in laboratories.

One of the best processes that we have selected is chemical absorption process in which biogas is upgraded to biomethane with the help of potassium hydroxide.

By this process, we have collected 55 tons/day biomethane as output, from 100 tons/day biomass feed. This biomethane is purified from traces like $H_2S$, $CO_2$ and $NH_3$. The overall process as shown in figure 3.1 we have treated 55 tons/day of biomethane with 10 tons/day of KOH as absorbent. The absorbent KOH can be regenerated after treating with the biomethane in the form of produced salts. This regeneration of the absorbents makes this process economical and feasible.

The overall process is simulated by using COCO/COFE software. The input data and stream line compositions are adjusted in the flowsheet of COFE software, and then run the simulation. Figure 3.2 shows the simulation of the overall process.



**Fig 6:** Simulation of the Overall Process

## 3.2 Individual Equipment Design Parameters

Design parameters such as length, diameter and volume for each equipment are calculated as shown in the table. These parameters are calculated by using residual time and L/D ratio, taken from literature and mass flow rate from material balances around each equipment.

The compressor used in this up-gradation process is Single stage compressor [19], which Compression Ratio is 5. Minimum RPM required for the compression is 672 and the power required for the compressor is calculated to be 0.94 kW

**Table II**: Equipment Design Parameters

| Equipment | Length (m) | Diameter (m) | Volume (m$^3$) |
|---|---|---|---|
| Anaerobic digester | 13.209 | 7.77 | 627.3 |
| Flash Chamber | 0.24 | 0.08 | 0.185 |
| Centrifuge | 3.84 | 0.48 | 3 |
| Absorption column | 7.2 | 2.06 | 3.33 |

## 3.3 Payback period

Total purchased equipment cost is calculated by estimating the purchased cost of each equipment, as shown in the table. Then total fixed cost for the whole plant was estimated. The values of several factors are taken from the literature.

**Table III**: Equipment Purchased Cost

| Equipment | Cost ($) |
|---|---|
| Anaerobic Digester | 6437 |
| Flash chamber | 3407 |
| Centrifuge | 232 |
| Compressor | 3277 |
| Absorption Column | 6353 |

The total fixed cost for the whole plant estimated is $ 90600. Other costs such as maintenance cost, labor cost, Raw material cost, plant overhead, etc. as a factor of total fixed cost are estimated to be $ 11453.

Taking Sale price as $ 0.45 / lge, [20], the payback period calculated for this plant is three years.

## 4. Conclusions

The biomass potential of Pakistan which is 853,500 tons/day can be utilized by using this process to generate 469,425 tons/day of bio methane. The technique used in this process for the up gradation of biogas to bio methane is environment friendly, as the H$_2$S gas is completely removed by treating the biogas with KOH absorbent. The waste from this process is a high-quality fertilizer, which is a byproduct of this process.

**Table IV:** Comparison Between Biogas and Bio Methane

|  | Biogas | Bio methane |
|---|---|---|
| Methane | 50-75 % | >97 % |
| Carbon dioxide | 25-50 % | < 3 % |
| Oxygen | 0-2 % | < 0.5 % |
| Hydrogen Sulfide | < 0-6000 ppm | < 5 ppm |

The cost of bio methane compared to other energy resources, charcoal, kerosene oil and firewood is 35 to 50 percent less. The deforestation rate can be control by using bio methane as a heating source. Pollution like water, soil and air can be reduced by converting organic wastes to bio methane. All these benefits make this process feasible and sustainable.

There are several reasons for not utilizing the biogas potential. Some major reasons of them are that there is lack of awareness of the peoples about this technology, lack of training facility in this regard and follow up to address these problems.

Production of bio methane can be enhanced by establishment of biomethane directorate

which will carry out the R&D activities regarding the improvement of this technology. Information regarding bio methane generation and advantages is to be disseminated through print and electronic media to develop awareness of the people about this technology. Conduction of training sessions will be helpful to share the technical aspects of this technology. Coordination with international experts will be more fruitful for the development of this technology.

## REFERENCES

[1] Amjid et all, 2011, "Biogas, renewable energy resource for Pakistan. Renewable and Sustainable Energy Reviews"; 15 (6), pages 2833-2837.

[2] Ellabban et al, 2014, "Renewable energy resources: Current status, future prospects and their enabling technology. Renewable and Sustainable Energy Reviews"; 39, pages 748–764.

[3] B.Bharathiraja et al, 2016 "Bio hydrogen and Biogas –An overview on feedstock's and enhancement process"; 810-828

[4] Iyyanki V.Muralikrishna "Environmental Management";Science and Engineering for Industry 2017, Pages 431-462

[5] Waqar Uddin et al, 2016 "Biogas potential for electric power generation in Pakistan: A survey"; pages 25-33

[6] www.blog.paksc.org, "Biogas can end Energy Crisis"; Retrieved October 2, 2016

[7] www.biomethane.org.uk, "What is Bio Methane"; Retrieved October 2, 2016.

[8] Wojciech M. Budzianowski, 2011, "Benefits of biogas upgrading to bio methane by high-pressure reactive solvent scrubbing, Biofuels", 6, pages 12-20.

[9] Alonso-Vicario et al, 2010, "Purification and upgrading of biogas by pressure swing adsorption on synthetic and natural zeolites. Micro porous and Mesoporous Materials."; 134, pages 100-107.

[10] E. Ryckebosch, M. Drouillon, H. Vervaeren, 2011, "Techniques for transformation of biogas to bio methane. Biomass and bioenergy"; pages 1633-1645.

[11] Pradeep et al, 2016, "Biogas Upgrading Technologies: A Review. International Journal of Recent Technology Science & Management", pages 2-4.

[12] Grazia Leonzio, 2016, "Upgrading of biogas to bio- methane with chemical absorption process: simulation andenvironmental impact. Journal of Cleaner Production"; pages 364-375.

[13] Pradeep et al, 2016, "Biogas Upgrading Technologies: A Review. International Journal of Recent Technology Science & Management", pages 2-4.

[14] H. Schultz et al, 2005, "Potassium Compounds in Ullman's Encyclopedia of Industrial Chemistry".

[15] Richard M. Feldar "Elementary Principles of Chemical Processes"; pages 635-637.

[16] Michael J. Moran & Howard N. Shapiro "Fundamentals of Thermodynamics"; pages 763-765.

[17] Abeam Khalid et al, 2011, "The anaerobic digestion of solid organic waste, Waste Management"; pages 1739-1744.

[18] Robin Smith "Chemical Process Design and Integration"; pages 17-33.

[19] www.gasequipment.com/catalogs/cryogenic/pdf/Blackmer/Compressors/Comp%20Selection%20and%20Sizing.pdf, "Steps to compressor selection and sizing"; Retrieved January 24, 2017.

[20] www.irena.org/costs/Transportation/Bio methane

# CFD Simulation of HAWT Blade and Implementation of BEM Theory

Muhammad Faizan Younas[1,] Awais Ali[1], Muhammad Abubaker[1], Muhammad Daud Shafique[1]

**Abstract:**

Wind turbine blade design is of profound importance in the renewable energy industry. This paper reflects a simple yet effective methodology to simulate a Horizontal Axis Wind Turbine (HAWT) blade. A blade of HAWT was designed with the implementation of the Blade Element Momentum Theory (BEM). With a Tip speed ratio (TSR) of 8, a blade of radius 10 m was designed with NACA 63-615 as a considered airfoil. In order to study the characteristics of flow over the designed blade, Computational Fluid Dynamics (CFD) simulations using ANSYS Fluent package were performed. Using frame motion, an unstructured mesh of around 2 million, and y + = 1, contours of pressure, velocity, and flow around the immediate vicinity of the blade were shown. The value of torque was found to be 5.6 kN.m for the designed blade. Lastly, a grid convergence study was done to find out the optimal size of mesh for this kind of simulation. Results clearly showed the efficacy of fluent package to model simulations of this type.

**Keywords:** *Blade Element Momentum Theory, Computational Fluid Dynamics, Tip Speed Ratio, ANSYS Fluent Package*

## 1. Introduction

Blade of a HAWT is of great importance for wind turbines. They can have myriad configurations in length, type and number of airfoils. Mostly blades are composed of a number of airfoils, instead of one, in order to ensure maximum lift at each section. BEM theory is a frequently used approach for the design of a HAWT blade. BEM is used by nearly all wind industries for the blade design and its optimization. It is a highly derivative form of Newton's second law of motion[1], and currently the only commercially available source for blade design. BEM theory considers a HAWT blade to be composed of a number of elements. With an input value of TSR, free stream velocity, lift

[1] Dpeartment of Mechanical Engineering, COMSATS University Islamabad, Sahiwal Campus, Sahiwal, Pakistan
*Corresponding Author: faizanyounas356@gmail.com

coefficient and design angle of attack (AOA), BEM

provides important design parameters i.e. twist distribution, chord distribution, and a relative tip speed ratio of every blade element [2-6]. In addition to the design process, by utilizing an iterative process BEM is also useful for the numerical computation of HAWT performance [7, 8].

In today's dynamic engineering environment, CFD is a burgeoning tool and has a broad spectrum of usage in myriad engineering fields. From modeling turbulence[9, 10], various chemical phenomena [11, 12], HVAC systems [13, 14] and all the way to the food industry [15, 16] CFD has proven potential. The following are some of the studies related to current work.

C. J. Bai et.al. [17] designed a HAWT with the application of BEM theory. Their study considered the National Renewable Energy Research Laboratory's (NREL) airfoil S822, a blade of radius 3m and an estimated output of 10kW. In addition, the improved BEM theory which includes Prandlt's tip-loss correction factor and Viterna-Corrigan stall model was used for performance prediction. In order to bolster the result, ANSYS Fluent package with k-ω SST turbulence model was used to verify the results obtained from BEM. A good agreement was found between results from BEM and that obtained from CFD simulations.

In a study conducted by Mehmet Bakirci [18], two airfoils i.e. NACA 64-421 and NACA 65-415 were taken under consideration. In order to find the OTSR (Optimum Tip Speed Ratio), six blade geometries were developed using of BEM at tip-speed ratios of 6, 7, and 8. For the analysis part BEM and CFD were deployed. A grid convergence study was also performed, with k-ω SST turbulence model the most accurate results were found at 2 million elements. The results shown a good agreement with BEM analysis, it is worth mentioning that in every case the maximum power coefficient

found at TSR greater than considered in design.

In order to find the starting torque behavior, a small HAWT was designed by Umesh et.al.[19], BEM was used for the design and analysis part. A computer program code with application of MATLAB was generated to predict performance. Moreover, ADAMS software was used in order to verify the results of BEM computationally. With a blade radius of 5 m, consistent values of torque were obtained after 5 sec.

In another study conducted by Emrah Kulunk et.al. [20], author designed a 100 KW HAWT with the application of BEM. The chosen airfoil was NREL S809, with 8.5 m blade and 9.43 m rotor radius. Moreover, a MATLAB program was also developed to predict the performance parameters like power, thrust, torque and coefficient of performance at wind velocities ranging from 10 to 100 m/s. Author also expounded on tip-loss correction factor for performance prediction. Results shown a direct relation between the wind velocity and performance parameters, but up to a certain limit this relation is not much dominant, and increasing velocities does not tantamount to performance increase.

A study was conducted to predict the performance of 150 KW HAWT numerically and experimentally by Yan-Ting Lin et.al. [21]. At different pitch angles the performance of HAWT with 10.8 m blade radius was investigated. Both BEM and CFD were deployed, with k-Ɛ turbulence model the best results were found at pitch angle 5°. Moreover, results obtained from CFD and BEM shown a good agreement. In a similar approach, effect of pitch angle on HAWT performance was studied by Sudhamshu et.al.[22]. At wind velocities of 7, 15.1, and 25.1 m/s ANSYS Fluent package with SST k-ω turbulence model was used to find best pitch angle. Results shown inverse relation of thrust coefficient with pitch angle.

Furthermore, for any given velocity optimum pitch angle was also studied.

A number of CFD studies were performed in past to investigate wind turbine performance. Lee et.al.[23] conducted study to investigate the effect of blunt airfoil on HAWT performance, with the application of ANSYS Fluent, HAWT blade were tested at different wind speeds. Results proven the blunt airfoil to be auspicious. Especially for small HAWT; mainly because they operate on higher TSR. Four methods for mesh independence study i.e. Grid Convergence Study (GCS), General Richardson Extrapolation (GRE), Mesh Refinement (MR) and Fitting Method (FM) was

investigated by Almohammadi et.al.[24] in case of a Vertical Axis Wind Turbine (VAWT). Results proven the fitting method to be best without any need for large mesh sizes.

A study was conducted by Moshfegi et.al. [25]. Using SST k-ω turbulence model the effect of near wall grid spacing was studied. Along the chord the separation point was found to be important factor after conducting 8 different cases, with element size no more than 5 million in every case. Similar studies that chronicles around different CFD techniques to study WT performance were describe in[26-34]

## 2. Methodoogy

### 2.1. BEM

For the implementation of BEM. The total length of the blade was divided into "n" number of elements, BEM treats every element as an independent member and provides design characteristics i.e. twist distribution and chord distribution that suits best at that member. In our case, the blade was divided into 10 elements with each of length 1 m. For the BEM implementation, the input parameters are given in Table-1.

**Table I:** Design parameters

| | |
|---|---|
| Lift coefficient ($C_l$) | 1.1094 |
| Blade radius (R) | 10 m |
| No, of blades ($N_b$) | 3 |
| Inlet velocity ($V_i$) | 10 m/s |
| Angle of attack ($\alpha_d$) | 5.0 |
| Tip speed ratio ($\Lambda$) | 8 |

Following steps detail the procedure followed to calculate blade design parameters with BEM theory:

Obtain local tip speed ratio for every element

$$\Lambda_r = \Lambda \left(\frac{r}{R}\right) \qquad (1)$$

where r is the local blade radius ranging from 1-10

Calculate optimum relative wind angle for every element

$$\emptyset_r = \frac{2}{3}\left(\tan^{-1}\frac{1}{\Lambda r}\right) \qquad (2)$$

Calculation of twist distribution

$$\theta = \emptyset_r - \alpha_d \qquad (3)$$

Calculation of chord distribution

$$C_{dr} = \frac{8\,P_{cf}\,r\,\pi\,\sin\emptyset_r}{N_b\,C_l} \qquad (4)$$

where $P_{cf}$ is the Prandlt's tip loss correction factor given by

$$P_{cf} = \frac{2}{\pi}\cos^{-1}[\exp(\frac{\frac{N_b(\frac{r}{R}-1)}{2}}{\frac{r}{R}\sin\emptyset_r})] \qquad (5)$$

At every element of the blade calculations were performed using above steps. Table-2 shows the output design parameters.

Fig. 1 shows the distribution of chord along the blade, as moving along the blade length, chord length decreases, same is the case with twist distribution and optimum relative wind

angle shown in fig. 2 and fig. 3. In contrast, local TSR increases along the blade length shown in fig. 4

**Table II**: Calculated design parameters

| Element Number | Local Radius $r$ (m) | Local TSR ($\Lambda_r$) | Twist Distribution ($\theta°$) | Chord Distribution $C_{dr}$ (m) | Relative wind angle $\emptyset_r$ ($\theta°$) |
|---|---|---|---|---|---|
| 1 | 1 | 0.8 | 29.22 | 1.327 | 34.22 |
| 2 | 2 | 1.6 | 16.34 | 1.05 | 21.34 |
| 3 | 3 | 2.4 | 10.08 | 0.791 | 15.08 |
| 4 | 4 | 3.2 | 6.57 | 0.622 | 11.57 |
| 5 | 5 | 4.0 | 4.36 | 0.509 | 9.36 |
| 6 | 6 | 4.8 | 2.85 | 0.429 | 7.85 |
| 7 | 7 | 5.6 | 1.75 | 0.371 | 6.75 |
| 8 | 8 | 6.4 | 0.92 | 0.321 | 5.92 |
| 9 | 9 | 7.2 | 0.27 | 0.261 | 5.27 |
| 10 | 10 | 8.0 | -0.25 | 0.197 | 4.75 |
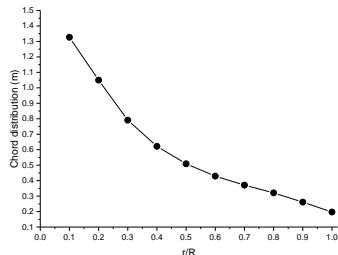


**Fig**. 1. Variation of chord distribution with blade length
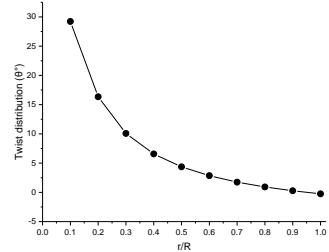


**Fig**. 2. Variation of twist distribution with blade length
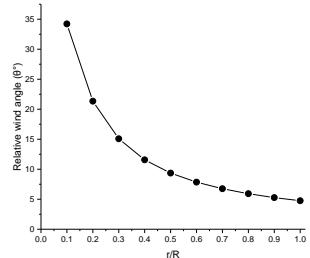


**Fig**. 3. Variation of relative wind angle with blade length
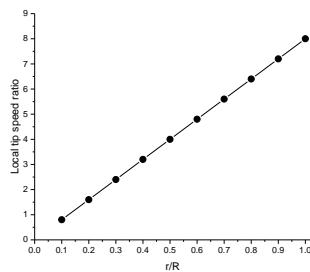


**Fig**. 4. Variation of local tip speed ratio with blade length

The calculated design parameters were used to create a CAD model in SolidWorks, the modeled blade is shown in fig. 5. It is worth mentioning that a hub radius of 0.5 m was assumed, but is not modeled in the present study as the only focus was to simulate the rotor.

To bolster the fact that we did not model the hub is because of its aerodynamic shape, which does not hinder the performance of the turbine, hence its effect can be neglected.
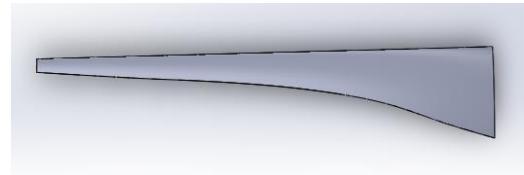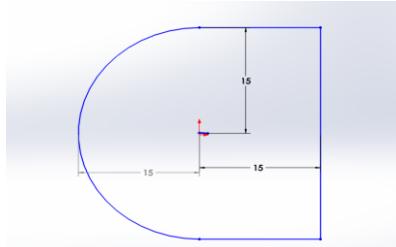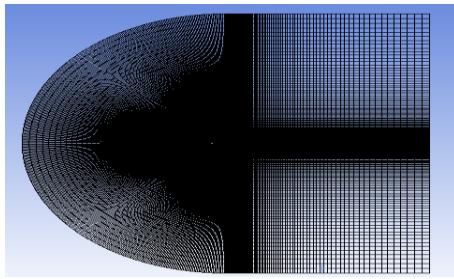


**Fig. 5**. CAD model of blade

### 2.2. CFD Analysis of Airfoil

Since airfoil $C_L$ is an input parameter so it is a good reason to perform 2D CFD analysis of the airfoil. 2D simulations were performed on an airfoil at 5° AOA, which is the maximum $C_L/C_d$ angle for this airfoil. A C-shape fluid domain was created with airfoil sitting in between the control volume Fig. 6.

**Fig. 6**. C-shape control volume

The boundaries of the control volume were extended 15 m from the airfoil, and the length considered for airfoil was 1 m. A structured mesh was created in the fluid domain after importing geometry in ANSYS Fluent. As shown in Fig. 7, the mesh was refined at the vicinity of the airfoil using a biasing function.



**Fig. 7.** Structured mesh around airfoil

The size of the mesh in Fig. 7 was around 100 K elements, as not much of variation in results was encountered upon increasing the size from 100 K.

Fig. 8 shows the structured mesh around the airfoil.
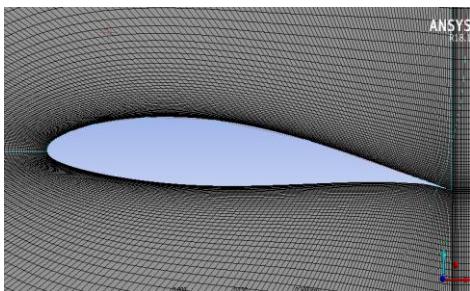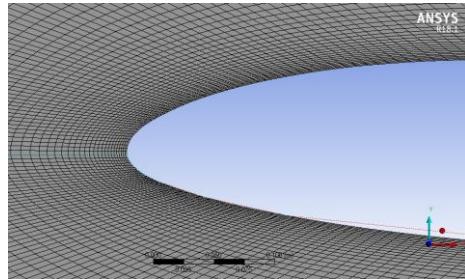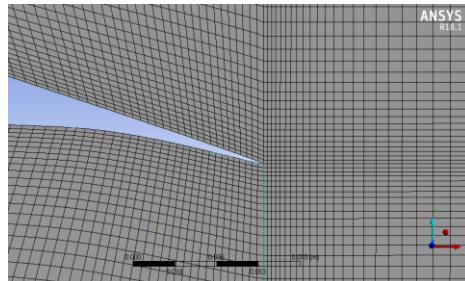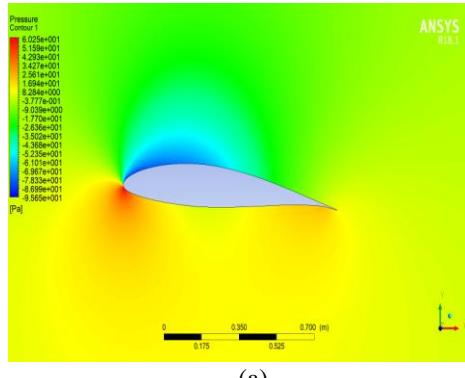


**Fig.8**. Structured mesh around airfoil

Fig. 9 and fig. 10 shows the mesh around leading and trailing edge of the airfoil.
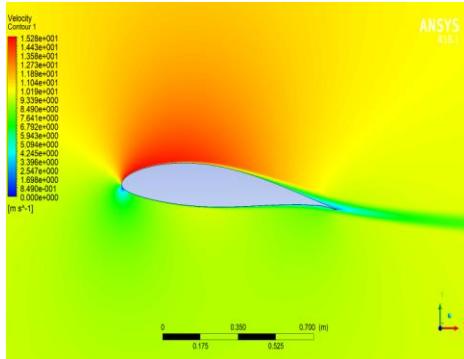


**Fig. 9**. Mesh around leading edge



**Fig. 10**. Mesh around trailing edge

With an inlet velocity of 10 m/s, the residuals of 1e-6 were set for 2D simulations. Because of the variation of the fluid velocity at the upper and lower side of the airfoil, a pressure difference was developed, and responsible for the lift creation.

Fig. 11 shows the pressure and velocity contours around the airfoil.



(a)

(b)

**Fig. 11**. (a) pressure contours around airfoil
(b) velocity contours around airfoil

### 2.3. CFD Analysis of HAWT

To simulate the rotor a pie-shape domain was created. With the simulation of a single blade, and implementing a symmetry boundary condition, complete rotor was analyzed. This little trick thus saved us time and computational resources. Fig. 12 shows a schematic of our designed control volume. Blade was placed at the center of the domain extended to 3R of the blade from inlet and outlet section.

Similarly, the inlet radius of fluid domain was 2R and 4R for the outlet. Fig. 13 and fig. 14 shows the actual mesh of control volume.
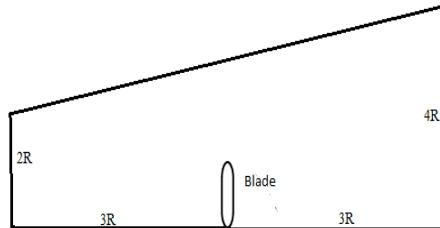


**Fig. 12**. Schematic of control volume
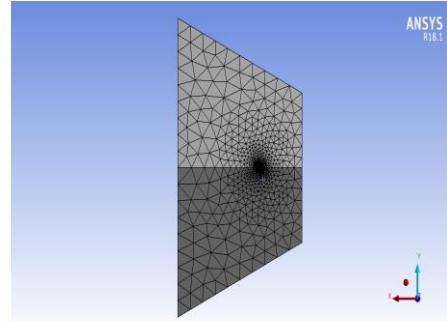


**Fig. 13** Mesh of control volume
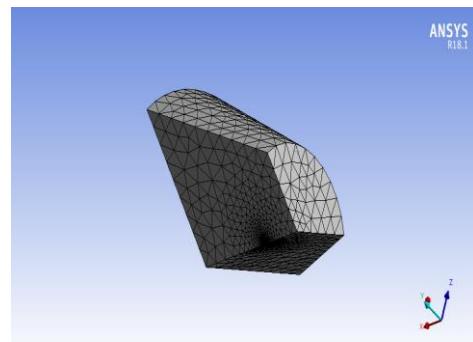


**Fig. 14** Mesh of control volume

An unstructured mesh with around 2 million elements was generated. In order to better capture the near wall viscous effects and shear forces a dimensionless wall quantity y + is used. y + is distance of the first computing node from wall. y + value varies with different turbulence

models, as for k ω-SST model it is generally, advice to keep y + < =1. k ω-SST is a two-equation eddy viscosity model and is highly effective in aerodynamics applications. It combines the benefits of both k-omega and k-epsilon turbulence models, hence well suited for flows in sub viscous layers and regions away from the wall [35].

Moreover, 27 layers of inflation were also part of the mesh, in order to better capture the viscous effects and shear forces near the wall. It may appear as a structured mesh around the airfoil, but these were the inflation layers

that wrap around the body to capture near wall effects. The mesh for this simulation contains tetrahedral elements only. A cut plane section of blade mesh is shown in fig. 15. and airfoil mesh is shown in fig. 16.
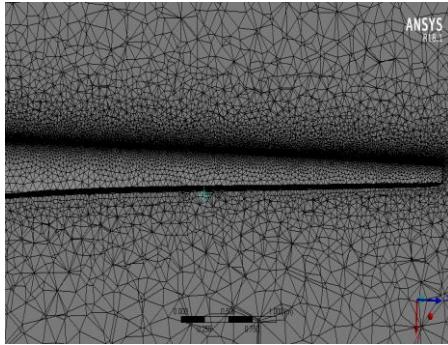


**Fig. 15**. Mesh around blade
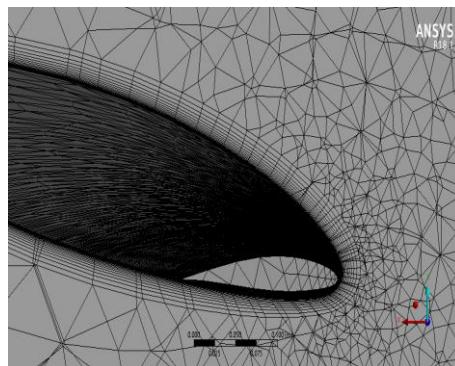


**Fig. 16**. Mesh around airfoil

Table-3 shows the boundary conditions considered for simulations.

As for the governing equations, Reynolds-averaged Naiver-stokes (RANS) equation was used to simulate the mean fluid flow given by

$$\frac{\partial \bar{U_i}}{\partial t} + \bar{U_j} \frac{\partial \bar{U_i}}{\partial x_j} =$$
$$\frac{1}{\rho} \frac{\partial \left[ -P\delta_{ij} + \mu \left( \frac{\partial \bar{U_j}}{\partial x_j} + \frac{\partial \bar{U_j}}{\partial x_i} \right) - \rho \overline{U_i' U_j'} \right]}{\partial x_j} \quad (6)$$

Where P stands for pressure, the term $\mu \left( \frac{\partial \bar{U_i}}{\partial x_j} + \frac{\partial \bar{U_j}}{\partial x_i} \right)$ are viscous stresses, $\bar{U}$ is the averaged velocity, $\rho$ is density, and $\rho \overline{U_i' U_j'}$ are the Reynold stresses. For modeling turbulence, turbulence model k-omega SST was used. The two-equation model is given by

**Table III:** Boundary conditions

| Boundary condition | Selection |
|---|---|
| Solver | Pressure based |
| | Absolute velocity formulation |
| | Steady state simulation |
| Fluid material | Air |
| Viscosity | 1.7894e-05 |
| Density | 1.225 |
| Temperature | 300 k |
| Pressure | 101,325 Pa |
| Wind speed | 10 m/s |
| CFD algorithm | Simple |
| Turbulence model | SST-kω |
| Cell zone condition | Frame motion of 2.3 rad/s |
| Wall condition | Moving wall |
| | No-slip shear condition |
| Solution methods | SIMPLE Scheme |
| | Gradient: Least square cell based |
| | Pressure: Standard |
| | Momentum: Second order up-wind |
| | Turbulent kinetic energy: First order up-wind |
| | Specific dissipation rate: First order up-wind |
| Solution controls | Pressure 0.3 |
| | Density 1 |
| | Momentum 0.7 |
| | Turbulent kinetic energy 0.8 |
| | Specific dissipation rate 0.8 |
| | Turbulent viscosity 1 |
| Mesh size | About 2000,000 |

$$\frac{\partial(\rho k)}{\partial t} + \frac{\partial(\rho u_j k)}{\partial x_j} = P - \beta^* \rho \omega k + \frac{\partial \left[ (\mu + \sigma_k \mu_t) \frac{\partial k}{\partial x_j} \right]}{\partial x_j} \quad (7)$$

$$\frac{\partial(\rho \omega)}{\partial t} + \frac{\partial(\rho \mu_j \omega)}{\partial x_j} = \frac{\gamma}{v_t} P - \beta \rho \omega^2 + \frac{\partial \left[ (\mu + \sigma_\omega \mu_t) \frac{\partial \omega}{\partial x_j} \right]}{\partial x} + 2(1 - F_1) \frac{\rho \sigma_{\omega 2}}{\omega} \frac{\partial k}{\partial x_j} \frac{\partial \omega}{\partial x_j} \quad (8)$$

Furthermore, continuity equation is given by

$$\frac{\partial \rho}{\partial t} + \frac{\partial(\rho u)}{\partial x} + \frac{\partial(\rho v)}{\partial y} + \frac{\partial(\rho w)}{\partial z} = 0 \qquad (9)$$

## 3. Results and Discussions

Fig. 17 shows the complete fluid domain. For our simulations, residuals were set to 1e-6, and the relaxation factors were set to default. Fig. 18 shows the residuals monitor for our simulation. 1500 iterations were done so ensure the maximum convergence, but it can be seen from residual plots that all the factors approached maximum convergence within 300 iterations, and solution didn't converge much afterwards. The tangential velocity was calculated by $v = \omega r$, as $\omega = 2.3\ rad/s$ is selected, the tangential velocity should be 23 m/s at the blade tip. Fig. 19 shows the velocity vectors on the simulated rotor, with a maximum velocity of 23 m/s at the tip. This is an important step in order to verify that our model worked well.
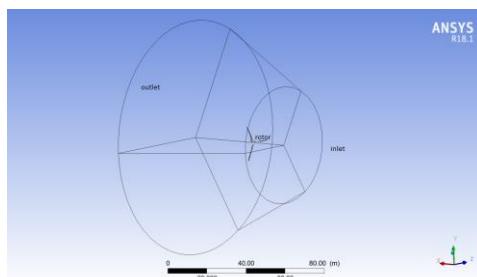


**Fig. 17**. Complete fluid domain
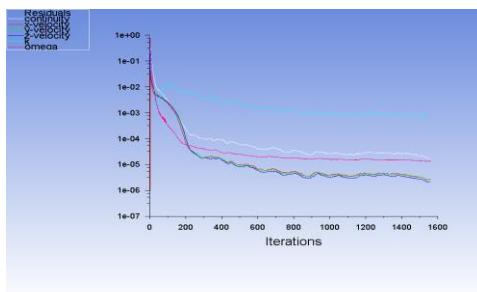


**Fig. 18**. Scaled residuals
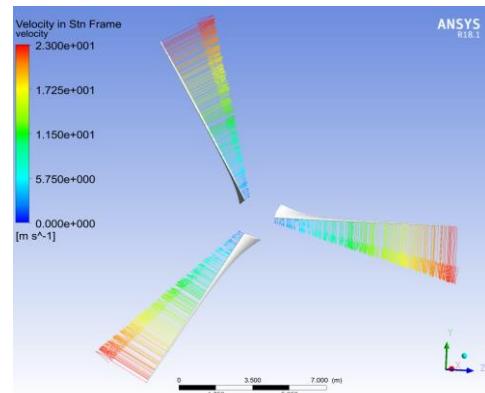


**Fig. 19**. Velocity vectors in Stn frame

Fig. 20 show the distribution of pressure contours along the blade length, the difference of pressure between both sides of the blade yields axial forces that turns the turbine. This axial force is directly related to the developed pressure difference.
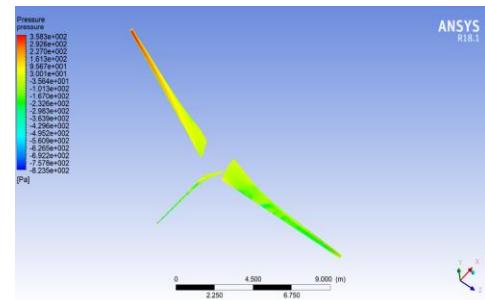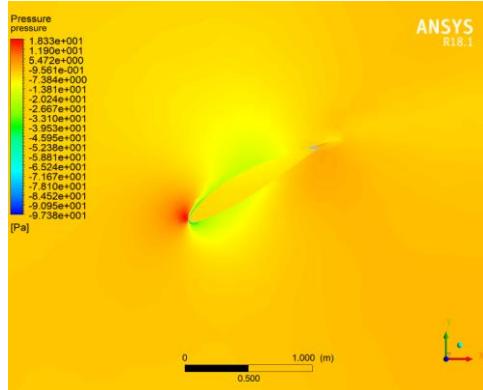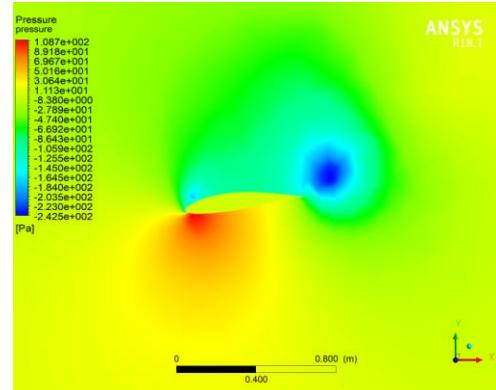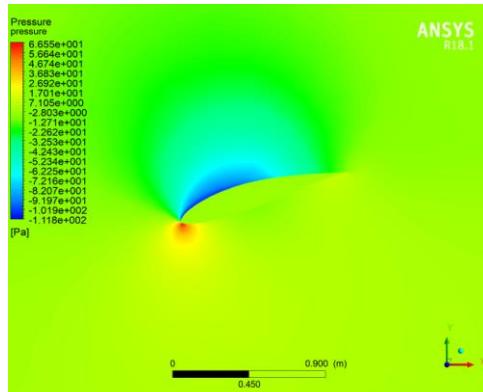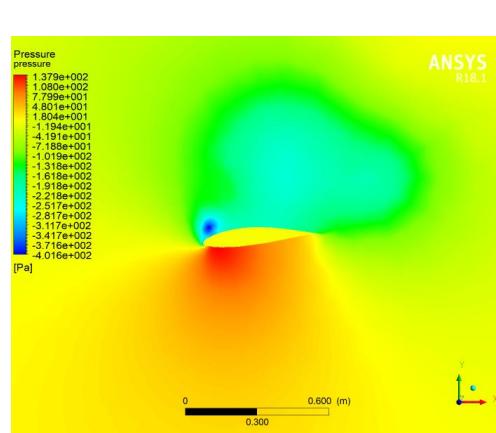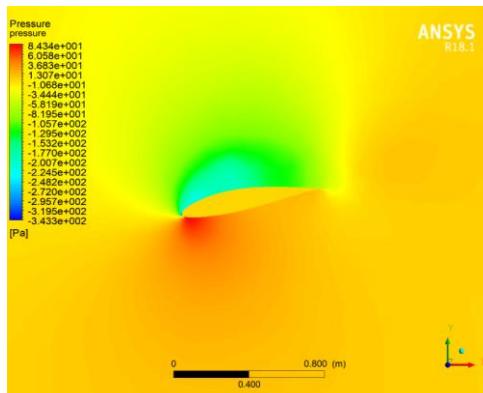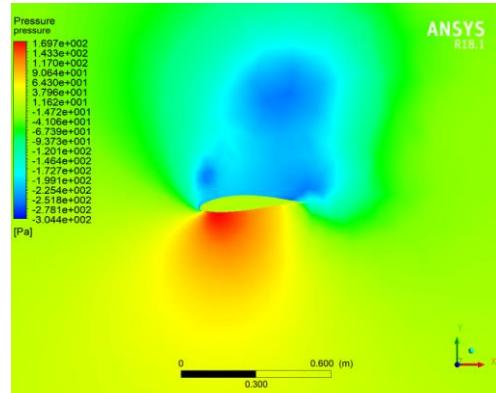


**Fig. 20**. Pressure contours on rotor

From fig. 21 - fig. 30. pressure contours at each blade element of blade are shown. It can be well observed that as moving along the blade pressure difference increases and every element contributes more to the rotation of the blade.

Minimum pressure was found 18.21 Pa at first element (r/R = 0.1) and a maximum of 351 Pa at the last element (r/R = 1) shown in fig. 31.

**Fig. 21**. Pressure contour at r/R = 0.1



**Fig. 22**. Pressure contour at r/R = 0.2



**Fig. 23**. Pressure contour at r/R = 0.3



**Fig. 24**. Pressure contour at r/R = 0.4



**Fig. 25**. Pressure contour at r/R = 0.5



**Fig. 26**. Pressure contour at r/R = 0.6
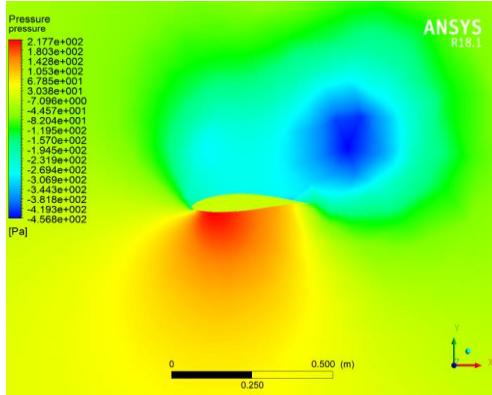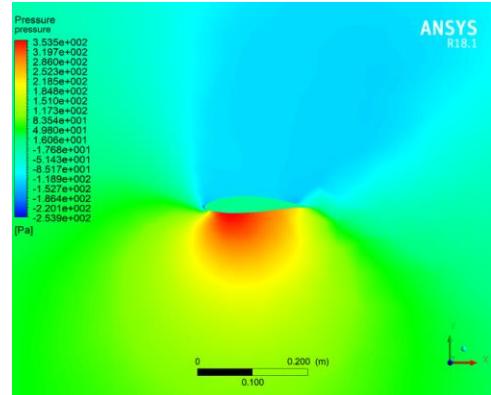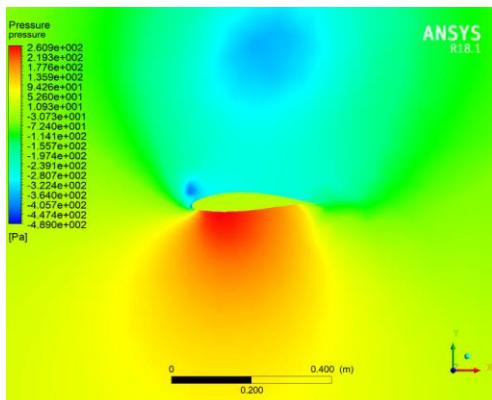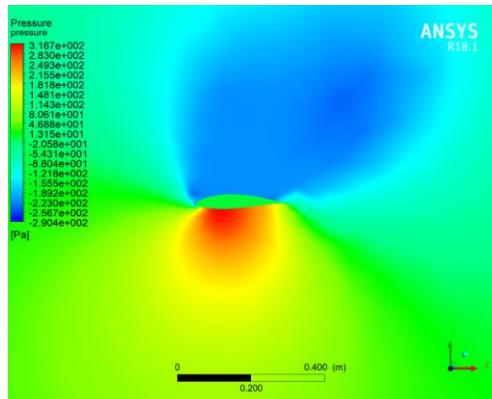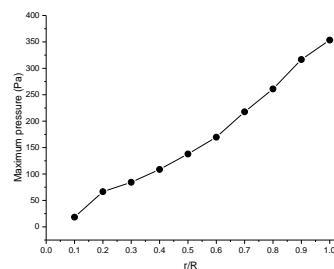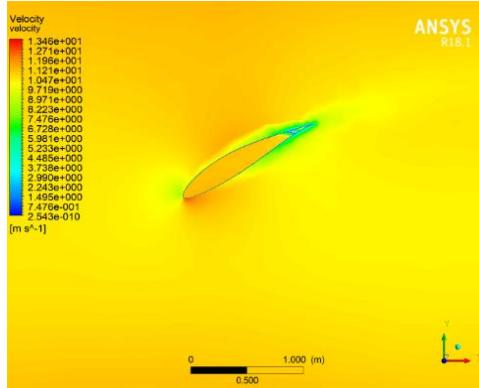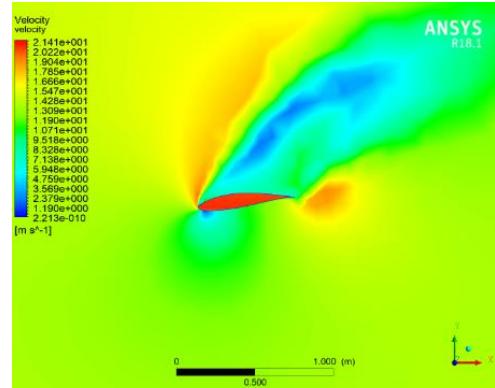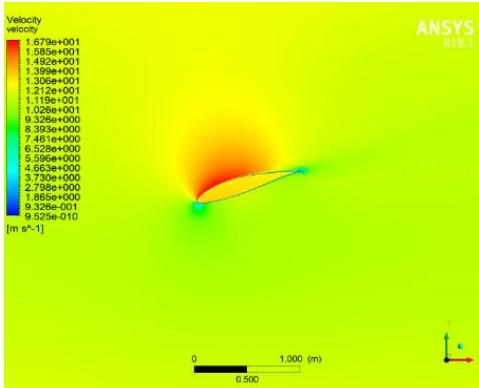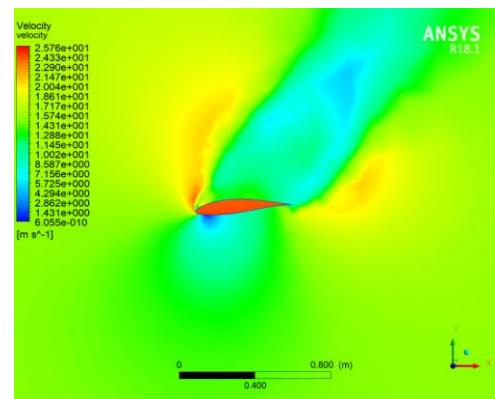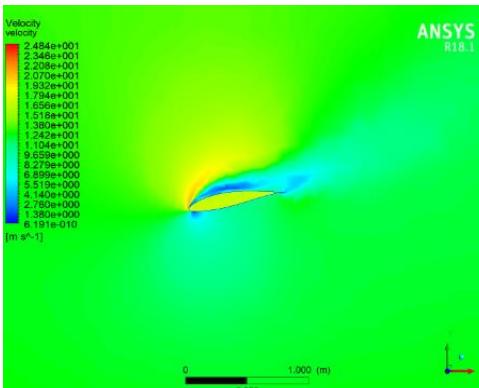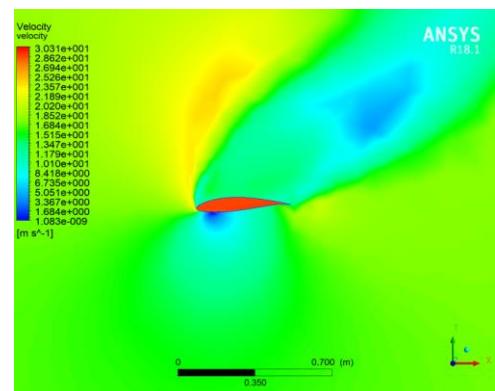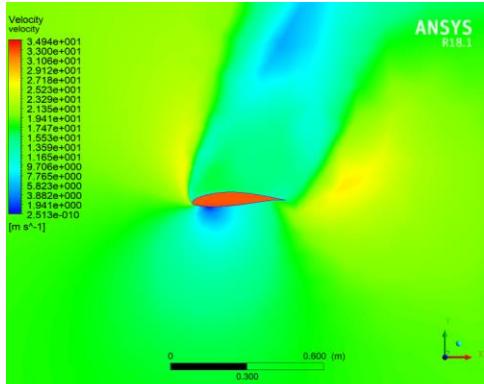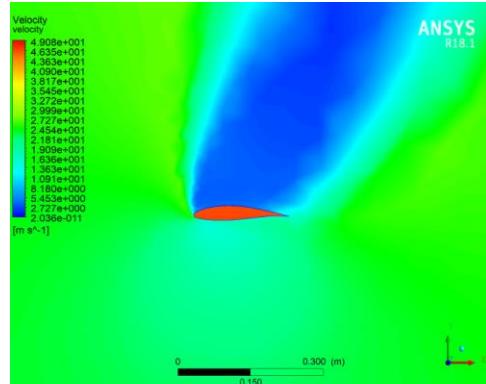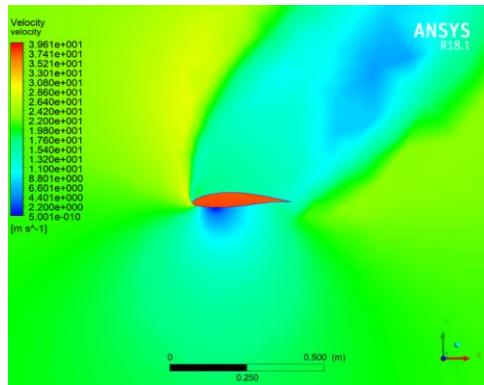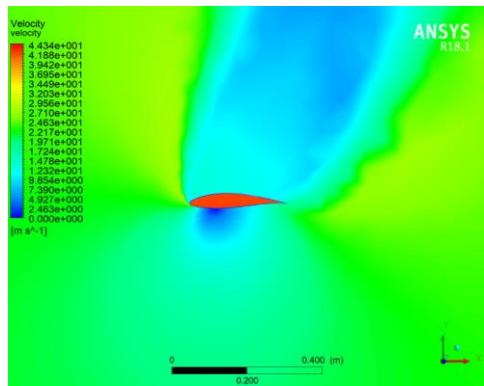
**Fig. 27**. Pressure contour at r/R = 0.7



**Fig. 28**. Pressure contour at r/R = 0.8



**Fig. 29.** Pressure contour at r/R = 0.9



**Fig. 30**. Pressure contour at r/R = 1.0



**Fig. 31**. Pressure distribution along blade

Similarly, from fig. 32 – fig. 41 velocity contours at each section of blade are shown. Like pressure, velocity contours become more aggressive as moving along the blade, with a minimum velocity of 15 m/s at first element and maximum of 31 m/s at tip section.
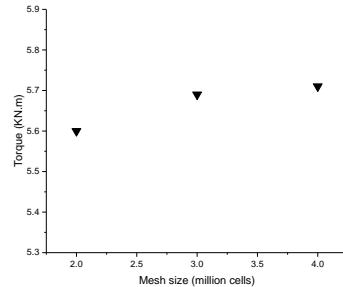
This rising trend is because of the decreasing angle of attack and chord distribution along the blade length.

**Fig. 32**. Velocity contour at r/R = 0.1



**Fig. 33**. Velocity contour at r/R = 0.2



**Fig. 34**. Velocity contour at r/R = 0.3



**Fig. 35**. Velocity contour at r/R = 0.4



**Fig. 36.** Velocity contour at r/R = 0.5



**Fig. 37**. Velocity contour at r/R = 0.6

**Fig. 38**. Velocity contour at r/R = 0.7



**Fig. 39**. Velocity contour at r/R = 0.8



**Fig. 40**. Velocity contour at r/R = 0.9



**Fig. 41.** Velocity contour at r/R = 1.0

Velocity contour at tip section (r/R = 1) shows the tip losses occurring at the blade. The torque value was also an important factor, at about 2 million mesh size the torque obtained was 5.6 kN.m.

A grid convergence study was done using the MR technique to find the optimum size of mesh for this simulation setup. The variation of torque with mesh size is shown in fig. 42. As not a clear nuance was found in torque value on increasing mesh from 2 million cells.



**Fig. 42.** Torque variation with mesh size

Due to the rotation of wind turbines, a disturbance in medium developed at the exit of the rotor known as wake effect. During the installation of wind farms, this phenomenon should take into consideration, so that the wake of one turbine does not hinder other's performance.

Fig. 43 shows the effect of the wake behind the moving turbine; the wake is maximum at the immediate exit from the turbine and a decline is observe as moving away from the rotor.



1m



2m
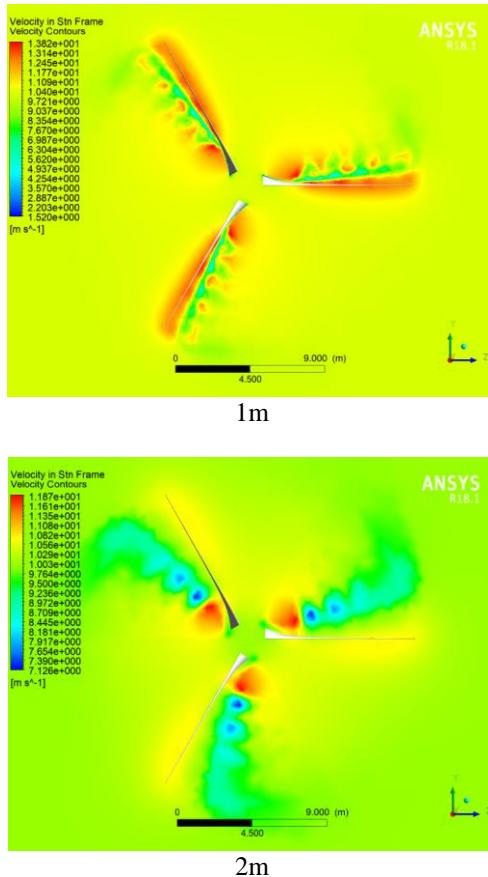
**Fig. 43**. Wake behind turbine at 1m and 2m

## 3. Conclusion and Future Work

A simple yet effective methodology was proposed to simulate the HAWT blade. Moreover, a mesh refinement study using the MR technique was done to bolster the results. As for future work, this methodology can be implemented on blades with somewhat complex geometries, and a comparison can be done to investigate how far the unstructured mesh holds to provide accurate

results. Furthermore, a juxtaposition of results can be done using different techniques of mesh independence study.

## Nomenclature

| | |
|---|---|
| $C_l$ | Lift coefficient |
| AOA | Angle of attack |
| CFD | Computational Fluid Dynamics |
| FM | Fitting Method |
| WT | Wind turbine |
| GRE | General Richardson extrapolation |
| MR | Mesh refinement |
| GCS | Grid convergence study |
| VAWT | Vertical axis wind turbine |
| R | Blade radius |
| RANS | Reynolds-averaged Naiver-stokes |
| $N_b$ | Number of blades |
| $V_i$ | Inlet velocity |
| $\alpha_d$ | Design angle of attack |
| $\Lambda$ | Tip speed ratio |
| $\Lambda_r$ | Local tip speed ratio |
| $\varnothing$ | Optimum wind angle |
| $\varnothing_r$ | Local optimum wind angle |
| $\theta$ | Twist distribution |
| $C_{dr}$ | Chord distribution |
| $P_{cf}$ | Prandlt's correction factor |
| $\omega$ | Rotational velocity |
| HAWT | Horizontal axis wind turbine |
| BEM | Blade element momentum theory |
| 2D | Two dimension |
| 3D | Three dimension |
| TSR | Tip-speed ratio |
| OTSR | Optimum tip-speed ratio |

**REFERENCES**

[1] M. O. Hansen, Aerodynamics of wind turbines: Routledge, 2015.

[2] F. Bohorquez, D. Pines, and P. D. Samuel, "Small rotor design optimization using blade element momentum theory and hover tests," Journal of aircraft, vol. 47, pp. 268-283, 2010.

[3] E. Kulunk and N. Yilmaz, "Hawt rotor design and performance analysis," in ASME 2009 3rd International Conference on Energy Sustainability collocated with the Heat

Transfer and InterPACK09 Conferences, 2009, pp. 1019-1029.

[4] E. Kulunk and N. Yilmaz, "Aerodynamic Design and Performance Analysis of HAWT Blades," in ASME 2009 Fluids Engineering Division Summer Meeting, 2009, pp. 1211-1222.

[5] R. Lanzafame, S. Mauro, and M. Messina, "HAWT design and performance evaluation: improving the BEM theory mathematical models," Energy Procedia, vol. 82, pp. 172-179, 2015.

[6] H. A. Madsen, C. Bak, M. Døssing, R. Mikkelsen, and S. Øye, "Validation and modification of the blade element momentum theory based on comparisons with actuator disc simulations," Wind Energy: An International Journal for Progress and Applications in Wind Power Conversion Technology, vol. 13, pp. 373-389, 2010.

[7] W. Duan and F. Zhao, "Loading analysis and strength calculation of wind turbine blade based on blade element momentum theory and finite element method," in 2010 Asia-Pacific Power and Energy Engineering Conference, 2010, pp. 1-4.

[8] G. Ingram, "Wind turbine blade analysis using the blade element momentum method. version 1.1," School of Engineering, Durham University, UK, 2005.

[9] J. Aubin, D. F. Fletcher, and C. Xuereb, "Modeling turbulent flow in stirred tanks with CFD: the influence of the modeling approach, turbulence model and numerical scheme," Experimental thermal and fluid science, vol. 28, pp. 431-445, 2004.

[10] Z. J. Zhai, Z. Zhang, W. Zhang, and Q. Y. Chen, "Evaluation of various turbulence models in predicting airflow and turbulence in enclosed environments by CFD: Part 1—Summary of prevalent turbulence models," Hvac&R Research, vol. 13, pp. 853-870, 2007.

[11] C. Yin, L. A. Rosendahl, and S. K. Kær, "Chemistry and radiation in oxy-fuel combustion: a computational fluid dynamics modeling study," Fuel, vol. 90, pp. 2519-2529, 2011.

[12] M. N. Kashid, D. W. Agar, and S. Turek, "CFD modelling of mass transfer with and without chemical reaction in the liquid–liquid slug flow microreactor," Chemical Engineering Science, vol. 62, pp. 5102-5109, 2007.

[13] J. Floyd, "Coupling a network HVAC model to a computational fluid dynamics model using large eddy simulation," Fire Safety Science, vol. 10, pp. 459-470, 2011.

[14] A. Patidar, S. Natarajan, and M. Pande, "CFD Analysis and Validation of an Automotive HVAC System," SAE Technical Paper 0148-7191, 2009.

[15] T. Norton and D.-W. Sun, "Computational fluid dynamics (CFD)–an effective and efficient design and analysis tool for the food industry: a review," Trends in Food Science & Technology, vol. 17, pp. 600-620, 2006.

[16] V. Chanteloup and P.-S. Mirade, "Computational fluid dynamics (CFD) modelling of local mean age of air distribution in forced-ventilation food plants," Journal of Food Engineering, vol. 90, pp. 90-103, 2009.

[17] C. Bai, F. Hsiao, M. Li, G. Huang, and Y. Chen, "Design of 10 kW horizontal-axis wind turbine (HAWT) blade and aerodynamic investigation using numerical simulation," Procedia Engineering, vol. 67, pp. 279-287, 2013.

[18] M. Bakırcı and S. Yılmaz, "Theoretical and computational investigations of the optimal tip-speed ratio of horizontal-axis wind turbines," Engineering Science and Technology, an International Journal, vol. 21, pp. 1128-1142, 2018.

[19] U. Chaudhary, P. Mondal, P. Tripathy, S. K. Nayak, and U. K. Saha, "Modeling and optimal design of small HAWT blades for analyzing the starting torque behavior," in 2014 Eighteenth National Power Systems Conference (NPSC), 2014, pp. 1-6.

[20] E. Kulunk and N. Yilmaz, "HAWT Rotor Design and Performance Analysis," pp. 1019-1029, 2009.

[21] Y.-T. Lin, P.-H. Chiu, and C.-C. Huang, "An experimental and numerical investigation on the power performance of 150 kW horizontal axis wind turbine," Renewable Energy, vol. 113, pp. 85-93, 2017/12/01/ 2017.

[22] S. A.R, M. C. Pandey, N. Sunil, S. N.S, V. Mugundhan, and R. K. Velamati, "Numerical study of effect of pitch angle on performance characteristics of a HAWT," Engineering Science and Technology, an International Journal, vol. 19, pp. 632-641, 2016/03/01/ 2016.

[23] S. G. Lee, S. J. Park, K. S. Lee, and C. Chung, "Performance prediction of NREL (National Renewable Energy Laboratory) Phase VI blade adopting blunt trailing edge airfoil," Energy, vol. 47, pp. 47-61, 2012/11/01/ 2012.

[24] K. M. Almohammadi, D. B. Ingham, L. Ma, and M. Pourkashan, "Computational fluid dynamics (CFD) mesh independency techniques for a straight blade vertical axis

wind turbine," Energy, vol. 58, pp. 483-493, 2013/09/01/ 2013.

[25] M. Moshfeghi, Y. J. Song, and Y. H. Xie, "Effects of near-wall grid spacing on SST-K-ω model using NREL Phase VI horizontal axis wind turbine," Journal of Wind Engineering and Industrial Aerodynamics, vol. 107-108, pp. 94-105, 2012/08/01/ 2012.

[26] J. M. O'Brien, T. M. Young, J. M. Early, and P. C. Griffin, "An assessment of commercial CFD turbulence models for near wake HAWT modelling," Journal of Wind Engineering and Industrial Aerodynamics, vol. 176, pp. 32-53, 2018/05/01/ 2018.

[27] C.-J. Bai and W.-C. Wang, "Review of computational and experimental approaches to analysis of aerodynamic performance in horizontal-axis wind turbines (HAWTs)," Renewable and Sustainable Energy Reviews, vol. 63, pp. 506-519, 2016/09/01/ 2016.

[28] R. Lanzafame, S. Mauro, and M. Messina, "Evaluation of the Radial Flow Effects on Micro HAWTs through the Use of a Transition CFD 3D Model – part I: State of the Art and Numerical Model Review," Energy Procedia, vol. 82, pp. 156-163, 2015/12/01/ 2015.

[29] A. Rezaeiha, H. Montazeri, and B. Blocken, "On the accuracy of turbulence models for CFD simulations of vertical axis wind turbines," Energy, 2019/05/16/ 2019.

[30] J. M. O'Brien, T. M. Young, D. C. O'Mahoney, and P. C. Griffin, "Horizontal axis wind turbine research: A review of commercial CFD, FE codes and experimental practices," Progress in Aerospace Sciences, vol. 92, pp. 1-24, 2017/07/01/ 2017.

[31] W. Miao, C. Li, G. Pavesi, J. Yang, and X. Xie, "Investigation of wake characteristics of a yawed HAWT and its impacts on the inline downstream wind turbine using unsteady CFD," Journal of Wind Engineering and Industrial Aerodynamics, vol. 168, pp. 60-71, 2017/09/01/ 2017.

[32] F. Carneiro, L. Moura, P. C. Rocha, R. P. Lima, and K. Ismail, "Application and analysis of the moving mesh algorithm AMI in a small scale HAWT: Validation with field test's results against the frozen rotor approach," Energy, vol. 171, pp. 819-829, 2019.

[33] Y.-J. Chen, G.-Y. Huang, Y.-C. Shiah, and Y.-L. Tsai, "Performance Prediction for Small Horizontal Axis Wind Turbine (HAWT) by Integrated Theory and Experimental Verifications," International Journal of Precision Engineering and Manufacturing-Green Technology, pp. 1-10, 2019.

[34] S. Sakaria, M. Tailor, and S. Joshi, "Modeling & Simulation Analysis of 800 kW Hawt," in ICTEA: International Conference on Thermal Engineering, 2019.

[35] F. R. Menter, M. Kuntz, and R. Langtry, "Ten years of industrial experience with the SST turbulence model," Turbulence, heat and mass transfer, vol. 4, pp. 625-632, 2003.

# Techno-Economic Analysis of Solar Thermal Water Heaters in Pakistan

Muhammad Aitezaz Hussain[1] and Sobab Khan[1]

**Abstract:**

In today's life, the first and important entity to live life with peace is the availability of the energy to humans in every aspect. And the prime source of the energy is the natural resources of the world, which is facing the major problems such as depletion with time due to which its price is increasing day by day and most importantly they are bringing the climate changes in the environment very rapidly [1]. So, taking into the account these issues it is highly recommended by the researchers to switch towards the sustainable and environment friendly sources for fulfilling the energy needs. That will decrease the burden on already low amount resources and also causes no harms to our echo system [1]. Coming towards the Pakistan Energy, Pakistan is going through the intense shortage of the energy and power having high gap of the demand and the supply. Our energy and power sector mainly depend upon the crude oil and fossil fuels which are already facing the shortage. The natural gas is main source of energy in the domestic, commercial sectors. But due to the poor management and yet undiscovered reservoirs the demand of gas is very high as compared to its supply. The situation in the winter gets worst when the demands get to its peak [2]. In lots of areas especially, rural areas there is no such facility of gas. So, people are cutting trees and use biomass, etc. for their energy needs. Also, Pakistani industrial sector such as Leather, Textile, beverages uses daily thousands of gallons of hot waters for its different process which are again highly dependable on the fossil fuels [4]. In this paper, the alternative approach has been adopted for these issues, the study has shown that the solar thermal energy can play a significant role in the Pakistan's geography.  A newly introduced technology for these issues highlighted above is the Solar Thermal water heaters. Two types of solar thermal water heaters Flat plate and Evacuated tube collectors have been discussed and compared. Both have their own pros and cons, which are discussed. Anyone can be used depends upon the consumer choice, availability and requirements, Environmental and Geographical Conditions. They both are totally Sustainable and works on the solar radiations with almost zero running cost. The analysis is being carried out on the comparison between Auxiliary heaters (gas) with the solar water evacuated type heaters. The cost saving, energy saving, payback period was found by the mathematical approach.

**Keywords:** *Sustaiable, Solar thermal Water heaters, fossil fuels, climate*

---

[1] Department of Renewable Energy Engineering US. Pakistan Center for advanced Study in Energy, UET Peshawar
Corresponding Author: aitizazk36@gmail.com

## 1. Introduction

For the last few years Pakistan has been facing a severe energy shortage. This problem hugely affected the daily routine and most importantly the economy of the country. [2,17]. The shortfall is around 5000 to 6000Mw due to which the rural areas are going through 12 to 16 hours of loadshedding while the urban areas are under 8 to 10-hour electricity cutoff [2]. And if serious initiatives on immediate bases aren't taken, this shortfall can increase in the upcoming years. Figure 2 shows the supply and demand of electricity by (NEPRA 2016).

Potential of renewable energy in Pakistan is very phenomenal due to its unique climate. Pakistan lies mostly on sunny tracks. So, it receives the humongous amount of. solar radiations annually. Solar energy is hugely spread and available in large amount throughout the country [1, 2]. On average Pakistan receives 4.45 to 5.83 kwh/m$^2$/day of the global radiation [2]. Even this minimum value of the average radiations 4.45 kwh/m$^2$/day is quite higher than the world average radiation which is 3.61 kwh/m$^2$/day. [2, 15].

So, it shows that Pakistan can get enough benefits of the solar energy and can fulfill lot of its energy needs using this free available technology. The recording of the sunshine in different parts of the country is being carried out by the isolation station installed in big cities like Lahore, Karachi, Peshawar, Islamabad Multan and Quetta. Given in Figure 1.

Pakistan has taken some good steps towards the harnessing the renewable energies source after the 2006 renewable energy polices. Some wind and solar power plants were started. Feasibility reports were studied. The figure 1 show the areas of the country which can be used for harnessing the solar energy at high level [2].

The idea of solar thermal water heaters has been introduced for the first time on commercial scales at one of the leather Industry [2]. The solar collectors were

evacuated tubes collector type used 400 m2 areas. The whole arrangement gives hot water up to 70 to 80oC with 10oC change to the inlet water which were already used boiler. After the cost analysis it has been found out that the system has saved the cost of fuel up to 33%. [2] After a few years, the setup was updated and extended. It means we can use it for our domestic Scale too, and it can give us 60 to 70 % saving annually [2].
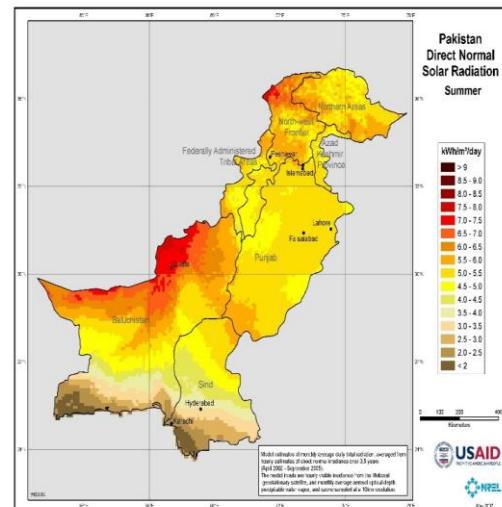


**Fig 1:** Direct Solar Irradiance of Pakistan.

This technology is very beneficial, cost effective, and clean and needs very negligible maintenance. But due to its high capital cost as compared to the conventional heaters, this technology isn't yet fully developed [3,4]. However, this is the most efficient technology and can be the best alternative for the areas where natural gas isn't available or deficient. Also, to the already decreasing natural resources and shortage of the power it is the best solution [2,12,18,].

## 2. Litreture Study

### 2.1 History

The history of use of solar heaters is very old. An inventor name Clarence Kemp in 1886 made a tank enclosed it in wooden box

which was first commercial type solar water heater [5], these heaters are still used and are now called Integral collector storage type heaters. [5] The Solar water heating technology was gradually growing and in 1920 the flat plate solar water heaters were introduced in Florida and South California, and were prominently used in America till 1960 [5]. After 1973 energy crisis, the technology grew abruptly. The developed countries like America, Japan, India, Canada Australia, Portugal, Spain and United Kingdom's widely opened their market to this technology. In the world Spain became the 1st country which used the solar photovoltaics and 2nd country for solar Thermal water heating technology in 2005 and 2006 respectively [5].
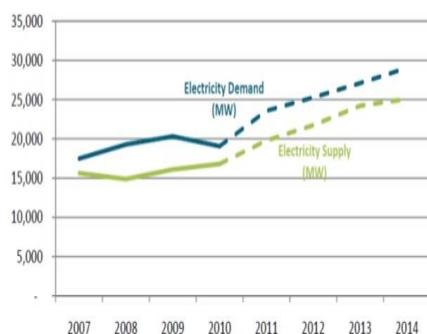


**Fig 2:** Demand and Supply Gap (NEPRA).
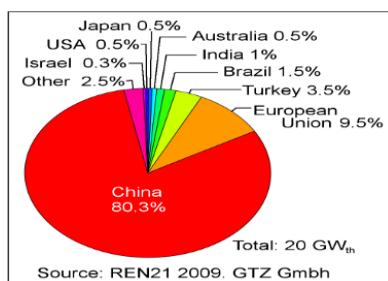


**Fig 3:** Pie graph shows the percentage Usage of worldwide solar water heaters up to 2007.

The technology is now also very common in China and its Products prices are very competitive in the market. Today prices of the normal solar heater in china are US dollar 235 which is approximately 80% less than the other countries prices. In China around 30 million household uses solar water heaters which is due to the advanced evacuated tube collectors' properties that can be used in cloudy sky or in cold climate with freezing temperature. After 1960 the market of solar thermal water heaters came into the Asia and Japan adopted this technology first [5].

## 2.2. Solar collectors

Anything that can convert the solar energy into the heat is supposed to be the solar thermal collectors [6]. Like the earth in self and the human body are also the clear examples of solar collectors. In more technical definition, the solar collector which helps to convert the incoming radiations of sun into useful form of heat and the example is warm air or water or any fluid. This principle can be simply realized by the hose pipe used to convey water for it and is also example of the simple unglazed collector. While minimizing heat loss from the system we used the glazed type solar collectors such as flat plat or evacuated tube collectors. The system can be further improved by using the concentrated collector with mirror which focuses the sun more on the collectors. The temperature of 3500 oC can be achieved in such method and the type is called solar furnace. [6, 19].
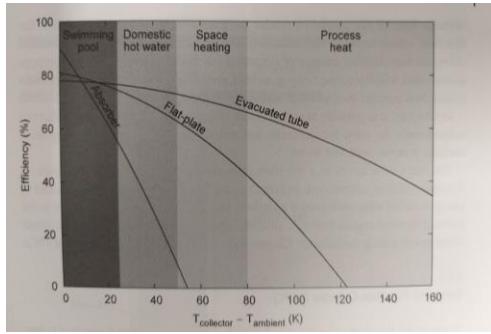
The performance of the solar collectors can be derived from actually taken heat Q with the incoming solar radiation G. So the efficiency of the collector can be found by equation (1).

$$\eta = \frac{Q}{G} \qquad (1)$$

Also, the Figure 5 shows that efficiency depends upon the operating temperature of the whole system [6].

Irradiation values for Pakistan, MJ/m$^2$ day

| Month | Karachi | | | Multan | | | Quetta | | | Lahore | | | Islamabad | | | Peshawar | | | Ben-ghazi, Libya, average |
|---|---|---|---|---|---|---|---|---|---|---|---|---|---|---|---|---|---|---|---|
| | Min. | Max. | Average | Min. | Max. | Average | Min. | Max. | Average | Min. | Max. | Average | Min. | Max. | Average | Min. | Max. | Average | |
| January | 9.6 | 17.7 | 15.3 | 6.0 | 15.2 | 12.2 | 5.9 | 17.6 | 13.2 | 4.6 | 14.2 | 10.5 | 4.6 | 14.1 | 10.1 | 4.4 | 15.6 | 10.5 | 11.2 |
| February | 10.0 | 19.8 | 16.3 | 6.9 | 18.8 | 14.6 | 7.4 | 21.7 | 16.0 | 5.7 | 19.1 | 13.8 | 4.4 | 17.5 | 13.6 | 5.3 | 19.9 | 14.3 | 13.0 |
| March | 11.0 | 23.7 | 20.2 | 8.8 | 23.2 | 18.0 | 9.0 | 25.1 | 18.9 | 7.6 | 23.4 | 17.6 | 5.7 | 21.9 | 15.5 | 5.8 | 24.8 | 17.4 | 16.6 |
| April | 15.9 | 25.0 | 22.2 | 13.5 | 26.2 | 22.5 | 12.9 | 29.6 | 24.2 | 10.8 | 26.0 | 21.6 | 9.7 | 27.2 | 22.0 | 10.4 | 28.0 | 21.5 | 20.2 |
| May | 17.0 | 26.4 | 23.0 | 13.9 | 27.4 | 23.6 | 15.0 | 32.1 | 27.4 | 12.4 | 27.7 | 23.1 | 13.0 | 28.1 | 24.3 | 13.2 | 30.1 | 24.9 | 24.1 |
| June | 14.2 | 27.4 | 22.5 | 13.2 | 27.1 | 22.8 | 21.2 | 32.0 | 28.6 | 12.8 | 28.0 | 23.6 | 13.5 | 28.0 | 23.3 | 16.5 | 31.2 | 26.5 | 24.1 |
| July | 10.4 | 25.6 | 17.5 | 12.4 | 26.3 | 21.6 | 15.2 | 29.6 | 24.9 | 8.4 | 26.5 | 18.9 | 10.8 | 27.3 | 21.1 | 12.6 | 28.7 | 23.2 | 26.3 |
| August | 9.8 | 25.6 | 16.8 | 13.5 | 25.3 | 21.4 | 14.8 | 27.6 | 24.1 | 9.4 | 25.9 | 19.5 | 10.1 | 25.3 | 20.5 | 9.1 | 26.2 | 20.9 | 24.1 |
| September | 11.6 | 24.6 | 30.1 | 14.1 | 23.2 | 20.2 | 17.9 | 26.1 | 23.1 | 11.9 | 23.7 | 19.8 | 13.4 | 2.1 | 19.5 | 3.2 | 23.4 | 19.2 | 19.4 |
| October | 14.2 | 21.4 | 18.9 | 11.9 | 19.6 | 16.7 | 13.7 | 22.9 | 19.7 | 10.6 | 19.2 | 16.0 | 8.9 | 18.4 | 15.7 | 9.1 | 19.2 | 16.0 | 14.8 |
| November | 11.5 | 18.1 | 15.7 | 9.6 | 15.9 | 14.0 | 8.6 | 18.8 | 15.3 | 7.2 | 15.0 | 12.4 | 7.8 | 14.5 | 11.6 | 7.0 | 16.7 | 16.3 | 12.2 |
| December | 8.2 | 15.8 | 14.1 | 5.9 | 13.6 | 11.1 | 0.2 | 15.2 | 12.3 | 4.7 | 13.1 | 10.2 | 3.8 | 11.7 | 8.1 | 4.6 | 13.1 | 10.5 | 43.2 |

**Fig 4:** Solar irradiations of different cities of Pakistan



**Fig 5:** Temperature Impact on Efficiencies of different Solar Collectors types

## 2.3 Water heating mechanism

The water heating mechanism is the circulation of water between the collectors and Storage tank or area where the water is used. Basically, there are two types of Heating water Mechanism [7].

### 2.3.1 Active system

This method used pumps, controllers and sensors for the water flow. It can be direct flow mechanism or indirect. In direct flow mechanism as the name suggests the water flows between the collector and the storage tank without any use of the heat exchangers. They are used in the area and perform efficiently where the temperature falls rarely below the freezing. While in indirect heating method the pump forces the water to flow between the collector then heat to exchanger A nonfreezing, nontoxic (propylene glycol) heating transfer fluid is used for this process. They are used in the area where the temperature falls below the freezing in colder climate. The active water heating system is more effective and works better than the passive system but due to high mechanical and controlling tools it's more expensive than the latter one. Figure 6 shows the circulation of the water through active system. [8].
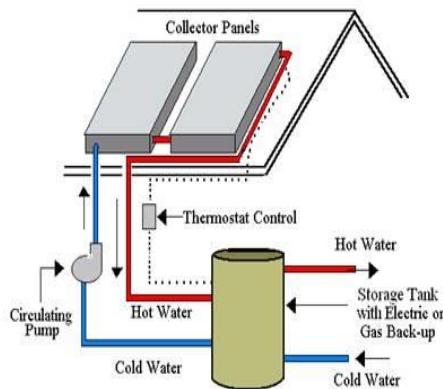
### 2.3.2 Passive system

In this mechanism the Circulation of water is through natural convection process. They are also of two types [8, 13].

### 2.3.2.1 Integrating collector Storage System

It uses a tank sealed within an insulated box. These tanks are thin rectilinear shaped while the side at which the glass in put on faces the sun side. the tanks acts as a collector and at the same time a storage as well. The water from the tank then heat-up though convection process and is available for use [9].

**Fig 6:** Active Solar Heater

### 2.3.2.2 Thermosyphon Process

This is also a natural process works on the simple physics principle, on the difference of the densities of the water. When water gets hot by the sun, it loses weight and gets rise [9].

While the colder water come to the bottoms of the collector. The risen water is then transferring to the storage taken or the header tubes which must have installed above the collector and so we don't need any tool or pumping system for the circulation of water in this system. The process of this system is shown in the Figure 7 [8]. These are the low temperature heater ranges from 40 to 80 degree above ambient temperature. So, they are mostly used for the domestic purposes where the average hot temperature is from 40 to 50 degree [8].
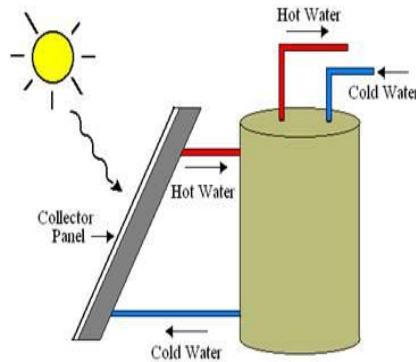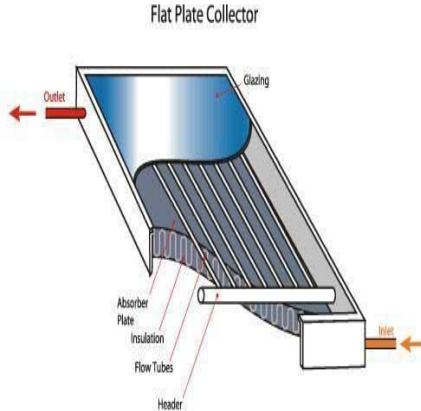
A metallic plate absorber plate which is made of cu, steel or aluminum. Mostly it is made of copper because of its higher conductivity as compared to the other two. It's also less corrosive.

## 2.4 Types of Solar Collectors

### 2.4.1 Flat Plate collectors:

The plate or the sheet is coated or painted black for high absorption Figure 8. Tubes are attached or the integral part of the plate which contains the HTF. The high transmittance glazing glass is used on the top

of the plate [12, 18]. The system is enclosed in the insulted box which prevent the heat loss from the Collectors backs and sides. They are fixed to the frame and so doesn't need any tracking**.** The efficiency of the flat plate solar collector is 45% [7, 21].



**Fig 7:** Passive Solar Water Heater



**Fig 8:** Flat Plat Collector

### 2.4.2 Evacuated Tubes Collectors

They are the latest technology-based collectors. And used on large scale for industrial applications where high temperature is needed up to 200 degrees centigrade [8].
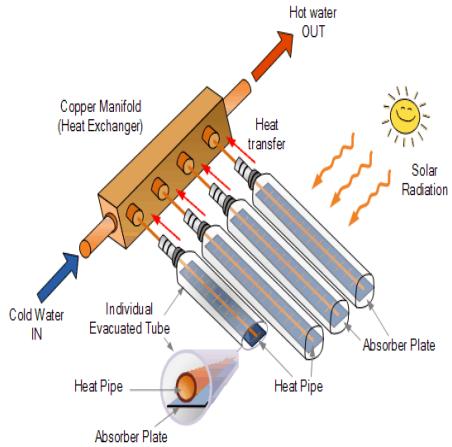
**Fig 9:** Evacuated tube Collector parts.

The Figure 9 shows the Structure wise parts. It consists of tube concentric glass tubes. The inner tubes with high absorptive coating contain the tubes having HTF. The outer tube is made of borosilicate glass which maximizes the transmission of the solar radiation falling on it to the absorbing plates or tubes. With the efficiency 80%, it can reach up to 120 degree above the ambient temperature [8]. Though the prices of evacuated tube collectors is high as compared to the former one, due to some exceptional properties they are surpassing the market worldwide. See Figure [10].

The evacuation or the removal of the air results vacuum creation between the two tubes which highly reduces the heat loss through convection or conduction. Also, the curve shape permits the tubes to collects the radiations from the large's angles and for long time of the day so high absorption of thermal energy occurs [11]. Due to these parameters it retains high temperature for long time. So, it could be efficient in colder regions or at nights. Solar thermal water heating technology becomes more prominent when the auxiliary heaters through electricity cost US dollar of 0.55/kwh and the gas cost at the rate of dollar 8.00/ MMBTU [7].
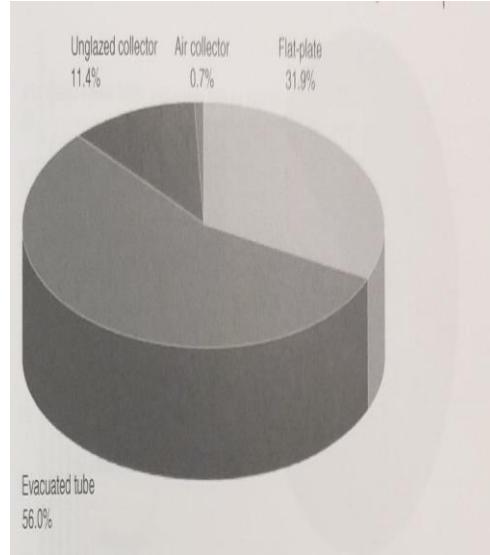


**Fig 10:** Shows the Global percentage Usage of Solar Collectors types.

## 3. Methodology

The Study of the paper is based on a leather industry which uses the evacuated tube collectors for heating purposes in different process. On industrial scale the hot water usage in leather and textile process is more as compared to the other. Study says that on the average the daily requirement of hot water for a leather industry is 120,000 liter/day at a temperature of 70 to 80 degree centigrade [4].

### 3.1. Design Requirements

Before going into the cost analysis. We should know about the technical and economic viability of a solar system which depends upon: How much sunshine is available throughout the year in particular area? What would be the capital cost of the solar system? What is the price of the conventional fuel [7]. The operational and maintenance cost of the system. What is the requirement of energy annually and how much the temperature of the hot water is desired. Apart from these basic parameters, we also need the rate at which the conventional fuel prices escalate. Taxes and other legislative issues must also be taken

into the account while designing of the plant for the area [7, 18].

The evolution procedure is being approached by the following method

### a. Estimating Daily hot water load

The daily hot water energy which could be consumed is given by:

$$L = MC (T_{hot} - T_{Low})  \quad (2)$$

Where

L= Daily hot water energy load in kwh/day

M= Mass of the water in kg/day

C= Specific Heat of water =0.001167 kwh/kg°C

$T_{hot}$= the temperature of the hot water which is to be deliver to the load (°C)

$T_{Low}$ = the temperature of the cold water which is to be given to the two collectors at input (°C)

Typical hot water Usage on domestic scale is 40 gallons/day/person and on industrial scale. let say a leather industry needs approximately 31700 gallons for tanning washing and bleaching of leather [4].

### b. Solar energy Resource

Collector should face south in northern hemisphere

Tilt angle: latitude of the areas (±15° for winter and summer respectively) [7].

### c. Solar water Heater system size

The size of the solar water heater system can be deducted by the following formula:

$$A_c = \frac{L}{nsolar \times Imax}  \quad (3)$$

Where;

Ac= area of collector in m

L= daily load in kwh/day

$\eta_{solar}$= efficiency of solar water heater collector

Typically, we take = 50 % for evacuated tube And 40% for flat plate [7].

### d. Annual Energy Saving

The amount of energy that could be saved annually is given by the formula:

$$Es = \frac{(Ac \times Iave \times nsolar)\,365}{nboiler}  \quad (4)$$

Where

*Iave* = average solar radiation of the particular area (kwh/m²/day)

$\eta_{boiler}$ = auxiliary heater efficiency

The study says gas heater efficiency is = 0.43 to 0.86. We will assume it 0.57.

While the electric heater efficiency is = 0.77 to 0.97. And we will assume it 0.88 (Source GAMA) [7].

## 3.2. Cost of Install Solar system

The installed system cost can be found by the following relation [7]:

$$C = c_{solar} \times A_c  \quad (5)$$

Where **C** is the total cost of the install solar system

And **C**$_{solar}$ = cost of the solar per unit area (m²)

**A$_c$** is the solar water heater system size respectively

### a. Cost saved annually

The total cost in annual basis can be calculated by the relation given [7]:

$$S = E_s \times C_e  \quad (6)$$

### b. Simple back period

The simple back period of the system can be finding out by the formula given below [7, 10].

$$SPB = \frac{C}{S}  \quad (7)$$

Where **C** is the cost of installed the system and **S** is the cost saved annually.

Where S is the annual cost saved

$C_e$ is the cost of the conventional or auxiliary energy.

For electricity NEPRA current rate Tariff.

### c. Tariff in Pakistan

Domestic Electricity Average Unit is PKR 15/Kwh. [17] while for Industrial its Average Unit is PKR 22/ Kwh. [17]

Similarly, for gas SNGPL Current rates are Domestic: [22]

Slab 1 = PKR 110/MMBtu for up to 1 Hm³

Slab 2 = PKR 220/ MMBtu over 1 to 3 Hm³

Slab 3 = PKR 600/MMBtu above 3 Hm³

While for Industrial Consumers (leather industries) its rate is PKR 600/ MMBTU [22].

In next Section the Mathematical equations explained in above section are applied on simple mathematical approach for Industrial and Domestic consumers both.

## 4. Results and Discussions

### 4.1. Cost Analysis for an Industry

As Already mentioned leather industry almost needs 120,000 liters of hot water at 60 to 70°C [4].

So, the industry selected has a setup for water heating through solar water heaters and having capacity of 90,000 liter of hot water at 10°C rise to the incoming water. Means if water comes at inlet at 50°C it will gets heated up to 60°C.

Applying the steps mentioned above:

#### a. Daily hot water load

$$L = MC (T_{hot} - T_{low})  \quad (2)$$

Total mass of water in kg:
1 liter = 0.264 gallons
Also 90,000 liter in kg = 89972 kg
So M = 89972 kg
C = 0.001167 kWH/kg°C
While as the $\Delta T$ is 10 °C.
Putting the values in equation (2) we get.
L = 89972$\times$ 0.001167 (10°)
L = 1050 KWH/day.

#### b. System size

$$A_c = \frac{L}{nsolar \times Imax} \quad (3)$$

Putting the values in equation we get,
$\eta solar = 0.50$ and $Imax = 5.5$ KWh/ m$^2$ for the region where the industry is Situated.
Ac = (1050$\div$ 0.50) $\times$5.5
Ac = 381 m$^2$

#### c. Annual Energy saving

$$Es = \frac{(Ac \times Iave \times nsolar) 365}{nboiler} \quad (4)$$

For gas heater we usually take the $\eta = 0.57$

To know about how much Energy has been saved per year, putting the corresponding values in equation (4), we get
Es = (381$\times$5.25$\times$0.50$\times$365) $\div$0.57
Es = 640430 KWH/year

#### d. Cost of install solar system:

$$C = c_{solar} \times A_c \quad (5)$$

Where $C_{solar}$ is the collector cost per unit area. In Pakistan for the larger units the cost ranges from 25000 to 40000 rupees. We would take 32000/= we get,
C = 30000 $\times$381m$^2$ = PKR 12192000/-

#### e. Annual Cost saving:

If we are using the gas as our auxiliary heater source. Then to find out how much cost has been saved we have the following equation:

$$S = E_{s} \times C_e \quad (6)$$

1 KWH = 0.00341 MMBTU
And 640430 KWH will be = 2185.86 MMBTU
At present as already mentioned above that Pakistan industrial rates are 600/MMBTU [22]. So, we get. Putting the values in equation (6)
S = 2185.86$\times$600
= PKR 1300000/ year approximately.

But as the gas is not sufficient enough to meet the demand of the country and there is obvious cut off of gas in winters. So the industries mostly relay than on Bio Fuel Like wood and Crops residues as there conventional sources of heat producing so that cost approximately RS 2200/- to produces 1 ton of steam. [14]

#### f. Simple payback period:

$$SPB = \frac{C}{S} \quad (7)$$

SPB = 12192000/1300000
$\approx$ 8 Years.

### 4.2. Cost analysis for a House

To look for the safety purposes on the domestic scale the solar water heaters must be used under the pressure relief value to supply and control the suitable temperature.

[8,14] The mixing or sometimes the tempering vales must be used if there is any possibility of the temperature reaching to highest point. the Figure 11 shows the typical two tank solar water heater collection in homes having the acceptable vales and pipe connections [8]. The Study says that the average use of hot water for one adult person per day is 40 gal/day. Hence for 4 family members' at least 160 gal/day would be required. [19]

Gas water heater can be storage for a time being or it could be used for instantaneous delivery. Load of water in kg /day would 160 gallons of water = 606 kg/ day.



**Fig 11:** Domestic solar Water heating system.

Let the inlet is 18º and the outlet we need 50º
So, applying the steps
As from equation (1)
 L = 606 × 0.001167(50º-18º)
 L = 22.6 KWH/day
Now as 1kwh= 0.00341 MMBTU
So, in MMBTU the total load would be = 0.077 MMBTU
From Equation 3:
Ac = (22.6÷0.50) × 5.5 = 8.2 m$^2$
From Equation 4:
Es = (8.2×5.25×0.50×365) ÷0.57
Es = 13783.55 Kwh/year
In MMBTU it would be = 47 units   ∵ 1 Kwh = 0.00341 MMBtu

As already mention that the domestic slabs from SNGPL the average MMBtu is around PKR 310/-
The total cost saving on yearly basis would be PKR 14570/-
For 4 family members on domestic scale single unit of the 300-liter capacity is enough. That is easily available in market from 30,000 to 60,000 depending on the quality and type. And the average cost of single evacuated tube collector could be 40,000/300lit. Taking the labor and other tooling cost (storage tank pipes etc.) cost may reach to 50,000 [8].
In last the simple payback period would be:
S = 50,000÷14570 ≈ 3 years.

## 5. Conclusion

So far important key points from the research have been derived. The best utilization proof of the solar thermal energy in Pakistan has been shown. The insolation in different area of Pakistan shows that this region is the best choice for the solar thermal energy on domestic as well as on industrial basis. In the calculation it has been shown that in the start capital amount need that may be the issue but onwards it's running and operational cost are almost free payback period has been cross. Hence it reflects how efficient and cost effective this technology is.

Moreover, it has not only potential to replace the conventional sources of energy for heating purposes but also it has that positive impact on environment as it reduces the carbon emissions in the air and optimally contribute to our ecosystem. A solar thermal water system has no production regarding the noise or air pollution. On industrial scale the solar thermal water heating has more viability in the sense of economics for larger use of collectors.

While on the Domestic scale it can decrease the gas as well as the electricity bill as shown in the calculation. This system can be more beneficial and efficient in the areas where no gas or electricity is present. For example, the northern areas of Pakistan and

Some areas of Baluchistan where either there is no gas or very rare.

The public use with an excess amount of bio wood or biomass for their energy needs, which both have negative impact on our environment as well as it takes lots of time and well power to fulfill the heating needs and totally relay on these conventional sources. So, the solar thermal water heaters are the best alternative for such areas as these regions have pretty high insolations high up to average of 8KWH/day/m2.

## REFERENCES

[1] Aized, T., Shahid, M., Bhatti, A. A., Saleem, M., & Anandarajah, G 45( 2018). Energy security and renewable energy policy analysis of Pakistan. Renewable and Sustainable Energy Reviews,84, 155-169. doi:10.1016/j.rser.2017.05.254

[2] Feasibility of a Solar Thermal Power Plant in Pakistan, Ihsan Ullah, Mohammad G. Rasul, Ahmed Sohail, Majedul Islam and Muhammad Ibrar , http://dx.doi.org/10.5772/55488

[3] Muneer, T., Maubleu, S., & Asif, M. (2006). Prospects of solar water heating for textile industry in Pakistan. Renewable and Sustainable Energy Reviews,10(1), 1-23. doi:10.1016/j.rser.2004.07.003

[4] Prosepect of solar water heating in textile industry https://www.dawn.com/news/369577

[5]Solarwaterheatinghttps://en.wikipedia.org/wiki/Solar_water_heating

[6] Duffie, J. A., & Beckman, W. A. (2013). Solar engineering of thermal processes. Hoboken: Wiley.

[7]NRELhttps://www.slideshare.net/khoised/course-solar-taylorthermal

[8] Hossain, M., Saidur, R., Fayaz, H., Rahim, N., Islam, M., Ahamed, J., & Rahman, M. (2011). Review on solar water heater collector and thermal energy performance of circulating pipe. Renewable and Sustainable Energy Reviews,15(8), 3801-3812. doi:10.1016/j.rser.2011.06.008

[9] Sootha, G. D. (1987). Solar Thermal Applications. Physics and Technology of Solar Energy,467-473. doi:10.1007/978-94-009-3939-4_19

[10]World Energy CouncilRenewable energy in South Asia: Status and prospects. London, UK; November (2000)

[11] Reduce Natural Gas Use in Your Industrial Process Heating Systems. (2007). doi:10.2172/915289

[12] Benz N, Gut M, Beikircher T. Solar process heat with non-concentrating collectors for food industry. In: Proceedings of Solar World Congress'99. 1999 [on CD ROM. p. 1209–14].

[13] Morrison, G. (1986). Performance Of Evacuated Tubular And Flat Plate Solar Water Heaters. Intersol Eighty Five,1184-1188. doi:10.1016/b978-0-08-033177-5.50230-1

[14] Muneer T, Hawas M. Experimental study of the thermosyphon and built-in-storage type solar water heaters. Proceedings of the energex '84 conference, Regina, Canada; 1984, p. 497–500 [ISBN: 0-08-025407-1]

[15] Hoskins, R., & Hirst, E. (1977). Energy and cost analysis of residential water heaters. doi:10.2172/7215177

[16]National Renewable Energy Lab; http://wwwnrel.gov/analysis/tech_cap_factor.html, National Renewable Energy Lab USA, September (2010)

[17] Currentpk. (2018, November 14). NEPRA decides Rs. 0.41 per unit hike in electricity tariff. Retrieved from https://currentpk.wordpress.com/2018/11/14/nepra-decides-rs-0-41-per-unit-hike-in-electricity-tariff/

[18] Huang J, Pu S, Gao W, Que Y. Experimental investigation on thermal performance of thermosyphon flat-plate solar water heater with a mantle heat exchanger. Energy 2010;35:3563–8

[19] Smyth, M. (2005). Domestic Solar Water Heaters. Water Encyclopedia. doi:10.1002/047147844x.dw13

[20] Muneer T. Effect of design parameters on performance of built-in-storage solar water heaters. Energy Convers Manage 1985;25:277–81

[21] Raja, I., & Twidell, J. (1990). Diurnal variation of global insolation over five locations in Pakistan. Solar Energy,44(2), 73-76. doi:10.1016/0038-092x(90)90068-n

[22] Asghar, N. (2016, December 24). Check SNGPL Sui' Northern Gas Bill Duplicate Bill Online. Retrieved from http://theworldnews.in/sngpl-sui-northern-gas-bill-online-check-print

# Enhancing Energy Efficiency in Temperature Controlled Dynamic Scheduling Technique for Multi Processing System on Chip

Hamayun Khan[1], Muhammad Yousaf Ali khan[1], Qaiser Bashir[2], Muhammad Usman Hashmi[3], irfan Ud Din[3] , Shahid khan[4]

**Abstract:**

Microprocessors designs consist of many micro level chips that reaches to a state where thermal upsurge occurs due to rapid processing of data and effect (reduce) their efficiency in many different aspects. That production of heat can cause disintegration which makes the chips disable of doing many functions they are assigned to perform. Embedded devices are designed to combine hardware and software, software integration can insert to hardware to perform some specific function. Multicore embedded devices are in different shapes and dimension. It has various applications on larger scale in networking and nuclear powerhouses to small multimedia players printers, automobiles, cameras mobile handset due to higher demand of power the energy becomes the major concern of the multicore devices for this a thermal aware scheduling algorithm has been proposed that consider the migration of load from higher state to that of lower state and considers all type of tasks and forecast them according to the priority by maintaining the previous history. The proposed technique also considers various thermal values by consulting the previous priorities of task on multicore systems. Migration policy is used to share load from one core to another the algorithm efficiently decreases almost 3°C temperatures at 40% utilization and the energy utilization is 221.3 J which is 3.12 % improved as compared to the global EDF.

**Keywords:** *Storm, Atmi, Dynamic Power Management, Dynamic Thermal Management*

## 1. Introduction

Now a day's systems are getting advanced and they are characterized as they have "real time" necessities to operate efficiently. In such embedded machines, the performance of the system does not consider those results that come at the end of complete simulation of a task in a multi-core system, but consider the duration during which the required results can be achieved [1]. Such kind of systems is generally recognized as "Real Time Systems". These systems are usually linked to such applications that need

[1] Department of Electrical Engineering, Gomal University, D.I.Khan, KPK, Pakistan
[2] Department of Electrical Engineering, The University of Lahore, Lahore, Pakistan
[3] Department of Computer Science, Superior University, Lahore, Pakistan
[4] United Consulting Services, D.I.Khan, KPK, Pakistan

to have a smooth operation for all the applications that required reliability and cannot afford any erroneous results in such real time systems all the deadlines meet at the accurate time and no chances for the system to miss its deadline. If a deadline is missed a failure as response can occur. These devices are called hard real-time systems a very common examples on larger scale for hard real time systems are avionics systems, textile industries, nuclear power plants, and also those devices that operates with wire systems established by present advanced automobiles [2, 3]. 'Figure 1 illustrates the block diagram of real time system'.

While on other side systems in which the real time limit exists, but the system has the ability to function weather a multi-core system missed the deadlines or either releases late. Such type of system is recognized as "Soft real time embedded system". These embedded devices are safer as compared to hard. If the time limit for each task is missed and yet the system is functional such systems are known as "Soft" real time systems. The performance of the system can be slightly disturbed and can affect the total performance of the system. Such systems can be used in networking of cellular systems [4]. While there is another system in which the missing of deadline is acceptable. In this case, the deadline of the task takes place. Then there is no improvement in the overall results either such systems are known as "firm" real time such systems that can afford delay of few seconds like a server of network that can afford delay. A usual Real time system can behave as hybrid. Sometime it behaves as "hard" real time, for which all the deadlines can meet according to their arrangements for the efficient and safe functionality of the system and some other embedded aspects like "firm" and "soft" real time where the infrequent failure is acceptable. There are few characteristics of RTES are as follow [5]. In real-time embedded systems the overall accuracy of

the system depends on both the useful accuracy of the system and also on time constraints. Real-time systems know about significant information of the application running on the system. Real time system depends on deadlines predictability and consistency. Fault acceptance characteristics. Hard, soft and firm are those real time systems that are commonly used everywhere and they are linked with a conventional multi-core system. These are further categorized in few other types like interactive real time that gives response to a user while the application is in running mode these types of embedded devices depend on time so the user can expect the response of the system well on time. In such cases the user can have a better system's speed and have a continuous process and have very less chances of missing a deadline such systems have almost the same characteristics like soft real time embedded systems. All through in this research work, the word "real time embedded system" is concerned with properties of an embedded systems and the real time. Those devices that are in real time embedded system category have a larger number of common characteristics. Real time systems have characteristics like embedded while embedded systems usually have characteristics like Real time on larger level or either on smaller extent [6].
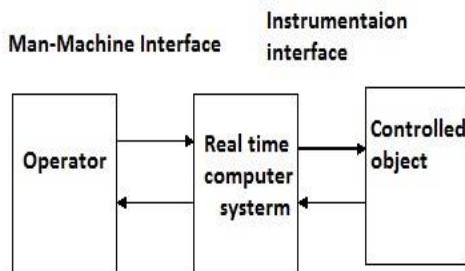


**Fig 1**: Block diagram of real time system.

### A. Events in Real-time Systems

In Real time systems events are categorize in two forms.

Synchronous Events: The release time assigned to all the tasks of an application is same.

Asynchronous Events: The release time assigned to all the tasks of an application is random. Figure 2 describes how a real time system works with synchronous and asynchronous events.
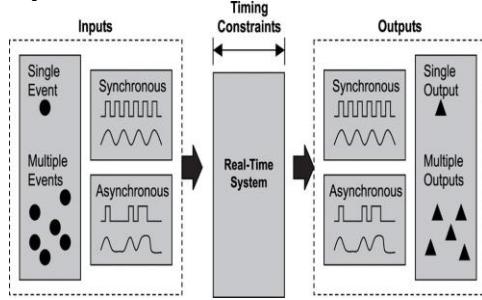


**Fig 2:** A simple view of real-time systems [7]

### B. Function of RTES

There are few functions of real time embedded systems. RTS, Nuclear power plants monitoring and scheduling, EMB, Printer, MP3 player and cell phone. RTSEMB Cardiac pacemaker.
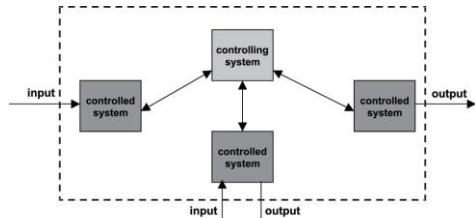


**Fig 3:** An Input/output Structure of Real time systems

RTES are those systems for which it is necessity to execute the set of jobs allotted to it firmly within the pre-set limit restrictions. Which is guaranteeing that all time-critical tasks are handled within time is called real time system with hard deadlines.

These tasks trust deeply on computational analysis and data plays an important role for achievement of the specific task to avoid scheduling issues all the resources that are distributed try to meet the time constraints for the task not to miss any deadlines [8].

## 2. Literature Review

Real-time systems are divided into hard and soft. The scheduling mechanism for hard are functional for soft real-time scheduling. Static and dynamic are the two further types of hard real time scheduling. The scheduling choices are usually occupied during the compilation time of task that depends on previous information about task set constraints [9]. Static scheduling occurs when the completing time for all the tasks are in the condition where scheduling by the scheduler finds earlier to the start of execution.

Tasks in which the information has some deadlines and the time for their execution is required are called static scheduling. The scheduling techniques occur during offline execution of tasks are static. In difference to this, dynamic scheduling makes quick decisions when the task is in running state by finding the set of tasks currently executing. This type of scheduling affords flexibility.

Dynamic scheduling represents such scheduling where the execution time for the task is not continuous and changes with time according to scheduler instructions.

During execution the process is completed dynamically when there is a limited priority assign to a task. In such order task are executing according to the plan settled during run time and deviates by the instructions provided from the scheduler. Executions of tasks with or without any issue are likely with both static and dynamic scheduling. Real time operating system proposed various scheduling mechanisms.

All these methods for scheduling have that issue that they allow prompt tasks to achieve execution by disturbing the execution of running tasks. All of them fall in the

classification of non-preemptive scheduling [10].

There are few Scheduling characteristics that are necessary for scheduling of a multi core real time system that are as follow [11, 12, and 13].

- Guaranteeing that system timing restraints are meeting.
- Avoid synchronized installment of devices and mutual resources.
- Attaining a state where utilization is very high.
- Confirms that the dispatch cost of a real-time systems must be low

Fundamentally, the scheduling problem includes expressing a plan for the implementation, execution and completion of all the tasks [14]. Due to advancement in embedded technology periodic activities shows more computational demand on a larger scale in a multi-core system these activities are categories in three types in a task model that are Periodic, A Periodic and Sporadic.

Figure 2-9 describes the various categories of jobs that are used in a processor' [15].
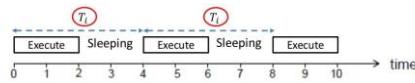


**Fig 4:** Categories of Task Model

## C. Periodic Task

In system monitoring periodic scheduling plays very important role periodic tasks usually occurs during control loops. These kinds of activities are continuously executing on definite rates. Periodic task repeats itself at specific periodic time interval in a continuous manner e.g. Control loops, Sensor reading [16]. 'Figure 5 illustrates how periodic tasks are scheduled for the completion of their jobs in a specified time.

For better Scheduling of task few notations are introduced that are as follow. For generic task sets i represents a periodic task while $T_i$

represents the time period of a general periodic tasks and øi represents the phase of task i. Tin represents the nth occurrence to a task "i" and Ria represents the release discharge duration for nth instance of task i in periodic task there are few major parameters that are used are written below. Reaction duration of an occurrence of task is the time in which the instance is finished. The time starts and calculates from the start of an instance to the discharge of a task at that time instance it is finished.

$Rak = fak - Tak-$

*Significant instant of a task:*

The time when larger response is created at the release of a job.

*Relation when release of a task occurs:*

Among two continuous instants the major deviation of change is known as relative release of a task.

$RRJa = max| (2i, fc-ra,fc) - (2i,fc-a-ra,fc-a).$

*Complete discharge jitter of a Job*

The instantaneous change in the duration between a single point instance and the maximum instant in which the deviation of a task occurs [43].

$ARJa = max (2a, fc – ra) - min (sa, fc – ra).$

There are three basic categories of scheduling algorithms that uses periodic tasks are Rate monotonic scheduling, earliest deadline first Scheduling and deadline monotonic scheduling.
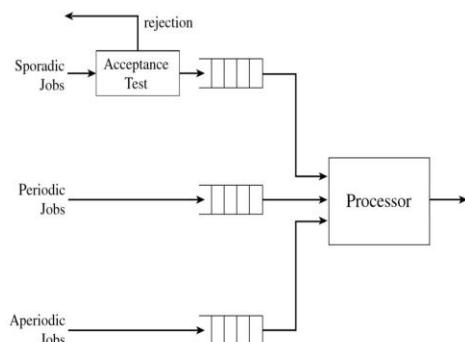


**Fig 5:** Periodic Task Model

## D. *A Periodic Task*

A periodic task can occur at any time interval when the task is in running mode. There is no specific instant for the occurrence of aperiodic task. Aperiodic task can have very elastic deadline and sometime aperiodic task doesn't have any deadlines e.g. Alarm clocks and all emergency embedded devices that can arrive at any time instant during emergency like robotic cars and obstacle avoidance system [17]. Figure 6 illustrates how aperiodic tasks are scheduled and jobs occur at any time instant.

## 3. Problem Statement

The main objective and focus of this research work is chip (reliability) that is the most important issues in multi core embedded technologies. High temperature causes multiple performances and reliability issues.
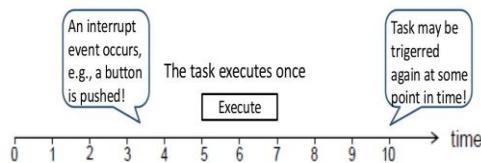


**Fig 6**: A Periodic Task Model [18]

Task migration is the way to avoid high temperature and improve performance. However accurate prediction about the coolest core and the task which needs to migrate to control the chip temperature is the major design issue in task migration techniques. Our technique considers all types of tasks including hot and cold task to accurately predict the temperature of the core in running mode and also use preciously thermal history to precisely check the chip temperature for the selection of cold core. A task migration technique based on previous history by considering workload of running core to predict the future temperature and coolest cores. This technique improves the reliability by avoiding thermal issues [19].

## 4. Experimental Technique

The major components include a task producer where user can create random task sets in XML file that contains different parameter. This XML input file is used as an input for the simulation tool. The simulation tool for real-time multiprocessor scheduling can simulate the input file according to the scheduling policy and developed the power profiles according to the set of parameters given in XML file. These Power profiles generated from STORM can be saved in a text output file. The XML file contains all the information of task sets. A temperature model can also analyze the thermal responses of different scheduling algorithms. A statistical testing mechanism is used to test a many data set. These data sets are already stored produces thermal profile when used with some hardware constraint in thermal model ATMI and a power model is used for each core comprises of static and dynamic power.

Total power = dynamic power + static power
*Dynamic power = C × F × V*
Therefore, C is the switching capacitance. F is the frequency and V is the supply voltage
Static power = Leakage current × V

### Flow chart

We have proposed technique for octa core multiprocessing Leat processor in which the scheduler will first check the number of task jobs as shown in figure 7.

That is running in an application. Primarily the value of counter is zero for all 8-cores in a multiprocessing leat processor. The scheduler is able to determine the constraint and values of every individual task. So, the counter for all the cores is initially zero. The configuration of core will be selected on the basis of least temperature and lower Power of consumption among all other configurations once the core with least temperature is

selected its counter in running mode is rapidly rising. In such case when the temperature of the core in running mode is less than the maximum allowable temperature then the scheduler will perform normal process of task execution.

parameter so only those cores are in running state that is in working condition. In the beginning exponentially, temperature on chip rises and then arrive at a steady state level. At 13% utilization factor the global EDF has 5°C more temperature on chip as



(c)

**Fig 8:** Thermal Cycling under 80Mhz for CPU1 & CPU2 at low Utilization Factor
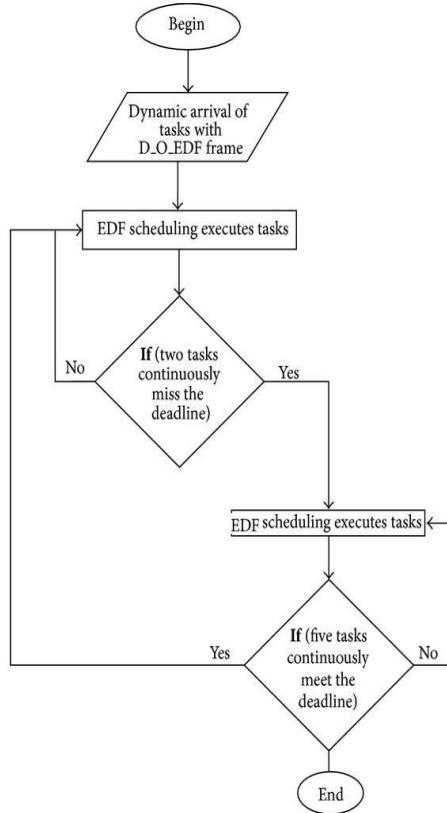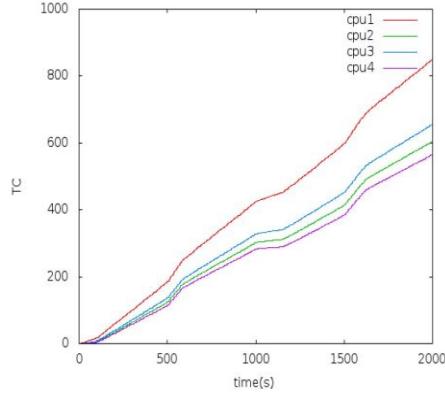


**Fig 7:** Flow Chart

## 5. Experimental Results
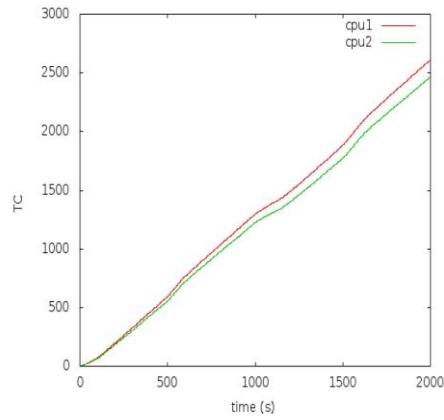
In this section we discuss our experimental results that illustrates the temperature variation between the curves of proposed EDF and Global EDF. Proposed EDF considers reliability and performance



(a)

**Fig 9:** Thermal cycling under 80Mhz for CPU1 & CPU2 at high Utilization Factor

(b)
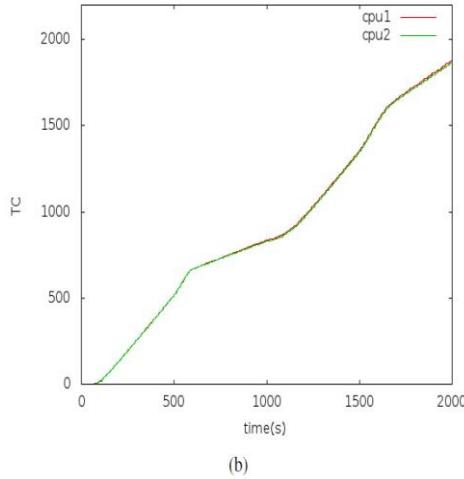
**Fig 10:** Thermal cycling under 80Mhz for CPU1, CPU2, CPU3 and CPU4 at low Utilization Factor



(d)
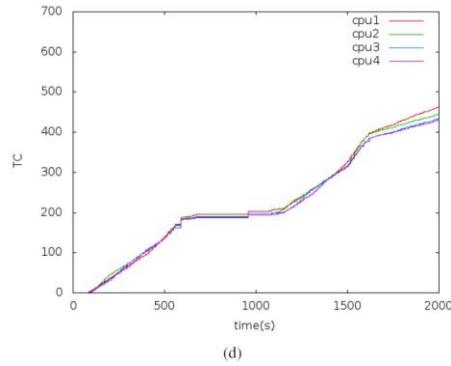
**Fig 11**: Thermal Cycling under 80Mhz for CPU1, CPU2, CPU3 and CPU4 at High Utilization Factor

## 6. Conclusion and Future Work

In this research work functional simulation on STORM and thermal model and proved its practicability in the context of MPSoC. A large amount of techniques now a days doesn't consider the affect of environmental temperature which can be investigated in future work. Majority of the current algorithms dsefines only for homogeneous multi-core systems which can be extensive to heterogeneous multi-core systems.

## REFERENCES

[1] Matt Bach. How ambient temperatures affect your pc. Temperatures-Affect-Your-PC-158/, Written on August 15, 2012.

[2] Shekhar Borkar. Design challenges of technology scaling. IEEE Micro, 19(4):23–29, July 1999.

[3] Thidapat Chantem, Xiaobo Sharon Hu, and Robert P. Dick.Temperature-aware scheduling and assignment for hard real-time applications on mpsocs. IEEE Trans. VLSI Syst., 19(10):1884–1897, 2011.

[4] Jian-Jia Chen, Shengquan Wang, and Lothar Thiele. Proactive speed scheduling for real-time tasks under thermal constraints. In Proceedings of the 2009 15th IEEE Symposium on Real-Time and Embedded Technology and Applications, RTAS '09, pages 141–150, Washington,DC, USA, 2009. IEEE Computer Society.

[5] H. Khan, M. U. Hashmi, Z. Khan, R. Ahmad, and A. Saleem, "Performance Evaluation for Secure DES-Algorithm Based Authentication & Counter Measures for Internet Mobile Host Protocol," IJCSNS Int. J. Comput. Sci. Netw. Secur. VOL.18 No.12, December 2018, vol. 18, no. 12, pp. 181–185, 2018.

[6] Farzan Fallah and Massoud Pedram. Standby and active leakage current control and minimization in cmos vlsi circuits. IEICE Transactions, 88- C(4):509–519, 2005.

[7] Stephen H. Gunther, Frank Binns, Douglas M. Carmean, and Jonathan C. Hall. Managing the impacincreasing microprocessor power consumption. (Q1):9, February 2001.

[8] H. Khan, M. U. Hashmi, Z. Khan, and R. Ahmad, "Offline Earliest Deadline first Scheduling based Technique for Optimization of Energy using STORM in Homogeneous Multi- core Systems," IJCSNS Int. J. Comput. Sci. Netw. Secur. VOL.18 No.12, December 2018, vol. 18, no. 12, pp. 125–130, 2018.

[9] Khan, H., Bashir, Q., & Hashmi, M. U. (2018). Scheduling based energy optimization technique in multiprocessor embedded systems. 2018 International Conference on Engineering and Emerging Technologies (ICEET).doi:10.1109/iceet1.2018.8338643

[10] Joohno Kong, Sung Woo Chung, Kevin Skadron, "Recent Thermal Management Techniques for Microprocessors" ACM Computing Surveys, Vol. 44, No. 3, Article 13, pp. 13:1-13:42, June 2012

[11] Mehdi Kamal, A. Iranfar, A. Afzali-Kusha, M.Pedram,"A Thermal Stress-aware Algorithm for Power and Temperature Management of MPSoCs" In EDAA, 2015.

[12] Q. Bashir, H. Khan, M. U. Hashmi, and S. Ali zamin, "A Survey on Scheduling Based Optimization Techniques in Multi-Processor Systems," in Proceedings of the 3rd International Conference on Engineering & Emerging Technologies (ICEET), Superior University, Lahore, PK, 7-8 April, 2016., 2016.

[13] T. S. Rosing, K. Mihic, G. De Micheli, "Power and Reliability Management of SoCs,"In IEEE Transaction Very Large Scale Integrated System (VLSI), vol. 15. no.4, pp.391-403, 2007.

[14]Pratyush Kumar,Lothar Thiele,"Thermally Optimal Stop-GO Scheduling of Task Graphs with Real Time Constraints,"In ASP-DAC, IEEE Press, pp. 123-128, 2011.

[15] Alexandru Andrei, Petru Eles, Zebo Peng, Marcus T. Schmitz, Bashir M. Al Hashimi, "Energy optimization of multiprocessor systems on chip by voltage selection," IEEE Transaction on VLSI, vol 50, no.3, 2007.

[16] "1965 – "Moore's Law" Predicts the Future of Integrated Circuits". Computer History Museum, 2007

[17] C. J. Lasance, "Thermally Driven Reliability Issues in Microelectronic Systems: Status-quo and Challenges". Microelectronics Reliability, pp. 1969–1974, December 2003.

[18] H. Khan, Q. Bashir, and M. U. Hashmi, "Scheduling based Energy Optimization Technique in multiprocessor Embedded Systems," in 2018 International Conference on Engineering and Emerging Technologies (ICEET). doi:10.1109/iceet1.2018.8338643, 2018.

[19] H. Khan, S. Ahmad, N. Saleem, M. U. Hashmi, and Q. Bashir, "Scheduling Based Dynamic Power Management Technique for offline Optimization of Energy in Multi Core Processors," Int. J. Sci. Eng. Res. Vol. 9, Issue 12, December-2018, vol. 9, no. 12, pp. 6–10, 2018.

[20] G. Petrone, G. Seagnuolo, R. Teodorescu, "'Reliability Issues In Photovoltaic Power Processing Systems", IEEE Transactions, July, 2008.

0.7"   Margin Top

# Paper Formatting Guidelines

## Title: 14pts Bold

## Author Name: 11pts Bold

*Affiliation: 11pts Italic*

**Abstract**: Single Paragraph (Min: 150 – Max: 250 words)

**Paper Length**: Formatted as guided (Min: 4,000 – Max: 8,000 words)

**Font**: Times New Roman 10pts

**Font Color**: Black

**Line Spacing**: 1.0 (single line space throughout the paper)

**Indentation**: Justify

**References & In-text Citations**: Follow the IEEE & Use EndNote X7 for In-text citations and Bibliography.

## Headings: 12pts Bold

1. **12pts Bold**
   1.1. **11pts Bold**
      1.1.1. ***11pts Bold Italic***

Margin Left                                                                        Margin Right
**0.8"**                                                                                      **0.5"**

# 6.5"x10"

*Page Size: 6.5" (Width) x 10" (Height)*

**Submission:** Formatted paper as guided can be submitted through our online submission system at http://sjet.iba-suk.edu.pk

**1.9"** | **Margin Bottom**

# Sukkur IBA
# Journal of
# Emerging Technologies

## Sukkur
# IBA
## University

## SUKKUR IBA UNIVERSITY
### Merit - Quality - Excellence